SAPIENZA UNIVERSITY OF ROME

SCHOOL OF BIOLOGY AND MOLECULAR MEDICINE

PhD THESIS

Functional studies of human K^+ channels KCNH1 and KCNK4 and their role in human pathogenesis

Human Biology and Medical Genetics PhD course

Medical Genetics curriculum

XXXII Cycle

Coordinator: Prof. Antonio Pizzuti

Tutor: Prof.ssa Viviana Caputo

Candidate: Dr. Giulia Napoli

A.A. 2018-2019

INDEX

ABSTRACT

Potassium (K^+) channels constitute the most diversified class of ion channels with regard to structure and gating characteristics. They contribute to the maintenance and stabilization of the resting potential and are key players in regulating cell excitability and functions in response to multiple signals (Tian et al., 2014). In recent years, the aberrant function of some of these channels has been documented to affect development and underlie syndromic disorders (Bauer et al., 2018).

KCNH1 (MIM 603305) is a member of the EAG (ether-à-go-go) family of voltage-gated K^+ channels (Cázares-Ordoñez and Pardo, 2017). Recent studies have demonstrated that gain-of-function mutations in KCHN1 are implicated in Zimmermann-Laband syndromes (ZLS; MIM 135500;Kortüm et al., 2015) and other forms of developmental deficits that include mental retardation and epilepsy (Simons et al., 2015;Bramswig et al., 2015; Mégarbané et al., 2016; Fukai et al., 2016). These findings suggest that KCNH1 might be important for cognitive development in human. Recently, gain-of-function mutations in *KCNK4* (MIM 605720), encoding a two-pore-domain K^+ channel (K2P), have been reported in subjects with a phenotype of facial dysmorphism, hypertrichosis, epilepsy, developmental delay/ID, and gingival overgrowth (FHEIG syndrome, MIM 618381; Bauer et al., 2018). The clinical features of the KCNK4-related condition are reminiscent of ZLS (Kortüm et al., 2015), providing evidence for a channelopathy caused by hyperactivation of K^+ channels, including KCNH1 and KCNK4.

Some ion channels are bifunctional proteins contributing to several cell functions (Hegle et al., 2006). To date, only electrophysiology experiments were performed to explore the mechanism involving KCNH1 and KCNK4 in ZLS and FHEIG related developmental processes (Kortüm et al., 2015; Simons et al.,2015; Bauer et al., 2018).

Based on these considerations, major aims of my PhD project were to better characterize the cell role of KCNH1 and KCNK4 channels and to explore the functional impact of the KCNH1-ZLS and KCNK4-FHEIG mutations using cellular and molecular biology approaches, including Immunofluorescence, Western Blot and Real-Time Quantitative PCR. To this aim, we used cell lines, control fibroblasts and primary skin fibroblasts derived from ZLS-patients carrying mutations in KCNH1 (p.Arg330Gln and p.Leu352Val) and from FHEIG-patients carrying mutations in KCNK4 (p.Ala172Glu and p.Ala244Pro). We demonstrated impaired proliferation of KCNH1 and KCNK4 mutant fibroblasts, confirming the role of KCNH1 as a regulator of cell cycle of non-transformed cells and highlight a new function for KCNK4 in regulation of cell proliferation. We also found a significant increase of cilia number and a cilium-related pathway, i.e. SHH pathway, activation in all the mutant fibroblasts, thus suggesting functional role of KCNH1 and KCNK4 in cilia regulation. Moreover, confocal microscopy analysis revealed defects in cilia morphology in fibroblasts from ZLS patients. Confocal analysis refined also the reported KCNH1 localization in the cilium (Sánchez et al., 2016) to be concentrated at the centrosome and ciliary pocket regions for both wild-type and mutant fibroblasts. Finally, immunofluorescence analysis conducted in

wild-type fibroblasts and cells lines disclosed a nucleolar localization of KCNK4 channels, possibly indicating unrevealed roles of KCNK4.

In summary, we demonstrated that KCNH1 and KCNK4 may have specific ion channel-independent function converging on some share cellular pathways whose alteration might affect development processes. Overall, these findings highlight the importance to characterize the intracellular role of K^+ to shed light on the mechanisms of pathogenesis of ZLS and ZLS related developmental processes.

1. INTRODUCTION

1.1 Human K^+ channels: cell functions

Ion channels are transmembrane proteins that regulate the flow of ions across biological membranes and are central regulators of the distribution of potassium (K^+), sodium (Na^+), calcium ($Ca2^+$), and chloride (Cl^-) ions for cellular ionic homeostasis. K^+ channels are the most diverse group of ion channels and are classified into four superfamilies, based on their domain structure and activation mechanisms, including voltage-gated K^+ (Kv) channels, Ca^{2+}-activated K^+ (KCa) channels, inwardly rectifying K^+ (Kir) channels, and two-pore domain K^+ (K2P) channels (Xi Huang et al., 2014).

The human genome contains almost 80 genes encoding K^+ channels, which constitute the most diversified class of ion channels with regard to structure and gating features. Such diversity allows K^+ channels to participate to many cell processes of both excitable and non-excitable cells. They control the K^+ flux through the cell membrane in response to multiple signals to modulate membrane potential and other cell functions. K^+ channels contribute to the maintenance and stabilization of the resting membrane potential, help to repolarize action potentials and mediate hyperpolarization. They are also key players in regulating cell excitability, cell volume, proliferation, apoptosis and cell cycle (Bauer et al., 2018). They also control neuronal information, muscle contraction and are important regulators of Ca^{2+}-triggered secretion of neurotransmitters and hormones. Furthermore, K^+ channels provide the driving force required for Ca^{2+} to enter the cell by keeping the membrane potential at hyperpolarized values. Ca^{2+} is an important mediator of intracellular signals implicated in the control of proliferation and other main cell processes (Urrego et al., 2014). Although different studies have shown that the expression and function of K^+ channels differ along cell cycle, the mechanisms controlling ion channels expression during the whole cell cycle remain elusive.

In proliferating cells, K^+ permeability determines the periodic changes of the resting membrane potential associated with each phase of the cycle. K^+ channels also play a role in cell volume changes required for the completion of mitosis and might influence signal transduction elicited by cell cycle checkpoints through protein-protein interactions or phospholipid clustering that modulates mitogenic signaling (Urrego et al., 2016).

Several studies showed that some voltage-gated ion channels are bifunctional proteins because they can also contribute to transcriptional regulation, protein scaffolding, cell adhesion and intracellular signaling, using mechanism independent of ion conduction (Hegle et al., 2006).

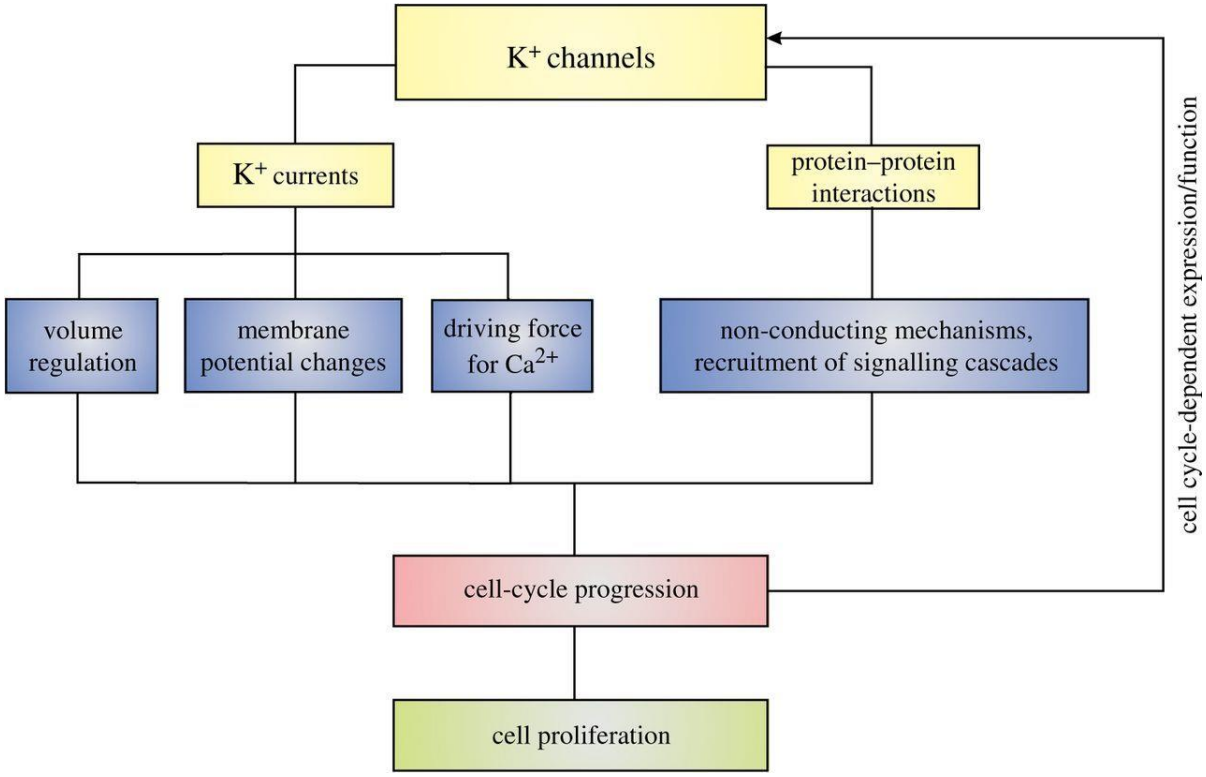

Figure1. K^+ channels in cell-cycle.

K^+ channels influence cell-cycle progression through cell volume regulation, modulation of membrane potential, generation of driving for Ca^{2+} and protein–protein interactions. K^+ channel expression or function can be in turn regulated by progression through the cell cycle (Urrego et al., 2014).

1.2 Potassium channels in human diseases

K^+ channels play important roles in a range of cell physiological processes and their aberrant activation or inhibition has been causally linked to altered neurotransmission, cardiac arrhythmias and endocrine and kidney dysfunction (Tian et al., 2014). Remarkably, the aberrant function of some of these channels has been documented to affect development and underlie syndromic disorders (Bauer et al., 2018).

K^+ channels are critical to neurotransmission in the nervous system and alterations in their function lead to remarkable perturbations in membrane excitability and neuronal function. Many neuronal disorders, such as episodic ataxia, benign familial neonatal convulsions, Alzheimer's disease, are related to mutations in K^+ channels (Shieh et al., 2000). Moreover, recent studies on K^+ channel gene expression in the basal ganglia, indicate that dysfunctions of several K^+ channels may be involved in the pathogenesis of Parkinson's disease (Tian et al., 2014).

There are many types of K^+ channels in mammalian cardiac cells, whose expression varies greatly throughout the heart, from atria to ventricles, from epi- to endocardium, and from apex to base. The critical role of K^+ channel dysfunction in cardiac arrhythmias is particularly evident in congenital channelopathies such as long-QT and short-QT syndromes, Brugada syndrome, and familial atrial

fibrillation, all associated with an increased likelihood of tachy-arrhythmias (Chiamvimonvat et al., 2017).

Besides neurologic and cardiac diseases, some diseases in other systems have been associated to K^+ channels dysfunctions. Permanent neonatal diabetes mellitus and type 2 diabetes mellitus are disorders associated with mutations in *KCNJ11*, encoding the Kir6.2 subunit of the KATP channel, and *KCNJ15*, encoding the inwardly rectifying K^+ channel, subfamily J, member 15, both involved in insulin release. Moreover, Bartter's disease, a familial salt-wasting nephropathy, is caused by mutations in the Kir1.1 channel, which mediates K^+ secretion and regulates NaCl reabsorption in kidney contributing to maintain plasma K^+ levels in the normal range (Tian et al., 2014).

There is increasing evidence showing that alterations in the expression of ion channels are involved in the progression and physiopathology of diverse human cancers. The roles of ion channels in cancer are differentiated and include regulation of cell proliferation, cell migration, cell volume control and apoptosis (Cázares-Ordoñez and Pardo, 2017). K^+ channels regulate cancer cell behaviors such as proliferation and migration through both canonical ion permeation–dependent and non-canonical ion permeation–independent functions. Highly proliferative cells are more depolarized than differentiated or quiescent cells. However, transient hyperpolarization is needed for progression during the first stages of the cell cycle. Therefore, a change in the membrane potential must occur for cell cycle progression, as well as during cell migration and adhesion and cytokine production against the tumor. K^+ channels would provide the driving force required for the Ca^{2+} influx that is necessary for cell cycle progression. At the same time, they may be involved in G1/S hyperpolarization, avoiding a loss of intracellular K^+ and preventing the cells from entering the apoptotic pathway. In addition to changes in Ca^{2+} homeostasis, apoptosis is characterized by voltage membrane decay and cell shrinkage, both related to the activity of K^+ channels (Serrano-Novillo et al., 2019).

1.2.1 Potassium voltage-gated channel subfamily H member 1 - *KCNH1*

KCNH1 (Kv10.1, Eag1, OMIM 603305) encodes the KCNH1 ion channel, a member of the Eag (ether-à-go-go) family of voltage-gated K^+ channels. In humans, *KCNH1* gene is located on the long arm of chromosome 1 (1q32.2). Alternative splicing of this gene results in two transcript variants (NM_172362.2 and NM_002238.3) coding respectively for two proteins of 989 (NP_758872.1) and 962 (NP_002229.1) amino acids, differing for an extracellular loop between the transmembrane helices 3 and 4 and encoding the same domains: the aminoterminal region, containing an eag domain, which is comprised of a Per-Arnt-Sim (PAS) domain and a PAS-cap domain, while the carboxy-terminal region, containing a cyclic nucleotide binding homology domain (CNBHD), and six transmembrane helices (S1-S6). The S4 helix works as a voltage sensor domain, the S5 and S6 helices are connected by the P-loop and together constitute the pore. Both the N- and the C-terminal domains are cytoplasmic and are necessary for the gating of the channel (Haitin et al., 2013). Additional splice variants were recently

identified, failing to form functional ion channels, but able to alter the glycosylation and expression patterns of canonical isoforms (Ramos Gomes et al., 2015).

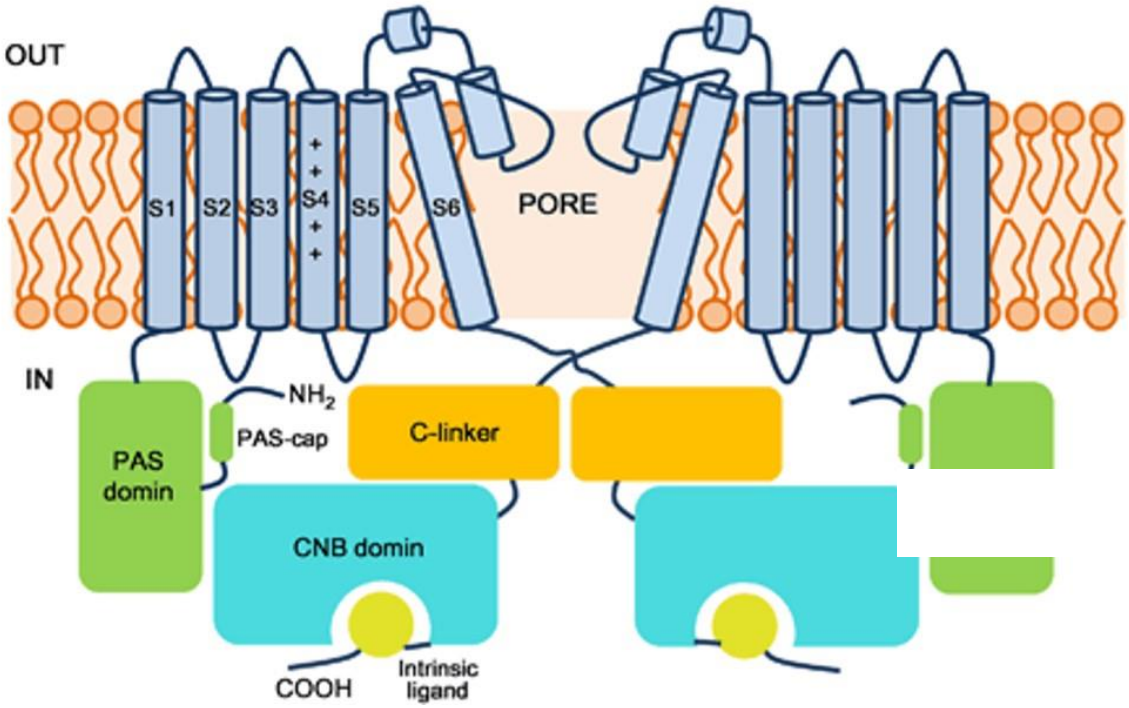

Figure 2. Schematic view of the KCNH1 channel showing the major structural domains.
The opposite two subunits are shown. Transmembrane domains are in light blue, the N-terminal PAS domains are in green, the C-linkers are in orange, and the CNB domains are in blue green. The intrinsic ligand motifs are highlighted in yellow (Haitin et al., 2013).

KCNH1 is highly expressed in adult central nervous system and in most human tumours, at low levels in placenta, testis, adrenal gland and transiently in myoblasts (Wang et al., 2017). It is aberrant expressed in cancer cells in contrast to its restricted distribution in healthy tissues. As its transforming activity and ectopic expression occurs in 70% of human cancers, KCNH1 is considered a clinically relevant ion channel and a marker and therapeutic target of several tumours. Cancer cells overexpressing *KCNH1* acquire selective advantages that promote cancer progression, such as chronic cell proliferation and migration, interference with oxygen homeostasis, regulation of cell cycle and modulation of ciliogenesis (Cázares-Ordoñez and Pardo, 2017).

KCNH1 is considered a bifunctional protein that, not only regulate K^+ flux, but also intracellular signalling pathways independent from its channel function. Non-cancer cells overexpressing KCNH1 show increased p38-MAP kinase (p-38MAPK) activity and p-38 MAPK inhibition abolishes the effect of the channel on cell proliferation (Hegle et al., 2006).

Cell functions of KCNH1 include the regulation of the resting membrane potential in both excitable and non-excitable cells, the modulation of cell volume and the regulation of proliferation and cell cycle (Urrego et al., 2014). Ion permeation does not seem to be a necessary condition for KCNH1 mediated proliferation and tumourigenesis, as non-conducting mutants retain the ability to influence both processes. In contrast, voltage-dependent conformations may be crucial for KCNH1 to support proliferation, as the non-conducting mutants in open conformation fail to influence proliferation. Channel blockers could reduce proliferation not only by inhibiting permeation but also by trapping the channel in a particular conformation (Urrego et al., 2014).

KCNH1 plays an active role in cell cycle progression in both cancer and non-transformed cells. In HeLa cells and mouse embryonic fibroblasts, KCNH1 depletion leads to delayed G2/M progression, indicating that channel expression at the end of the cell cycle facilitates G2/M completion. Functional studies performed in breast cancer cells also demonstrated that KCNH1 regulates the progression of cell cycle from G1 to S phase. Cells synchronized in G0/G1 shows increased KCNH1 mRNA levels accompanied by membrane hyperpolarization towards the S-phase and defective checkpoint control between G1 and S-phase. The expression of KCNH1 is coupled to cell cycle not only in cancer but also in normal cells, in which is temporally restricted to a time period immediately prior to mitosis. Moreover, KCNH1 promoter contains an E2F1-responsive element that during the G2/M phase is directly regulated by the activation of E2F1 pathway promoting cell cycle progression (Urrego et al., 2016).

The peak of KCNH1 expression during G2/M phase, which coincides with the time of disassembly of primary cilia, and its interaction with proteins that participate in ciliary regulation, such as Rabaptin 5 and cortactin, allowed to hypothesize a role for the channel in ciliogenesis (Sánchez et al., 2016).

KCNH1 is important for the neuronal excitability and is expressed in different brain regions in both rodents and humans but its physiological function remains poorly understood. Morphological and behavioral analysis were performed in KCNH1 knock-out mice to investigate the functional role of the channel in the brain and indicated that deletion of KCNH1 does not produce functional alterations in brain or severe cognitive or behavioral effects (Ufartes et al., 2013).

Mutations in *KCNH1* have been recently associated to Zimmermann-Laband syndrome (ZLS; MIM 135500; Kortüm et al., 2015) and also reported in Temple-Baraitser syndrome (TMBTS; Simons et al., 2015; Mégarbané et al., 2016), in unrelated individuals with intellectual disability (ID, Bramswig et al., 2015) and in individuals with syndromic developmental delay, hypotonia and seizures (SDDHS, Fukai et al., 2016), suggesting that *KCNH1* might be important for human brain physiology and cognitive development.

KCNH1 channels are homotetramers, with each subunit composed of six transmembrane helices. In ZLS cases, five of six KCNH1 mutations are located in the two helices (S5 and S6) involved in the opening of the channel and one mutation maps in the voltage-sensor helix (S4). All variants are single-nucleotide substitutions causing missense mutations, with a germline origin. A homology model for the S5 and S6 helices of KCNH1 was used to study the structural impact of p.Gly469Arg, p.Ile467Val, p.Leu352Val and

p.Val356Leu mutations. The p.Gly469Arg change is predicted to impair tetramer formation or favor the open state with a lower conductance by inserting four cationic residues close to each other in the closed state of the homotetramer. The p.Ile467Val, p.Leu352Val and p.Val356Leu substitutions are predicted to affect the closed-open transition. These residues form a tight hydrophobic cluster in the open structure which rearranges in the closed conformation (Kortüm et al., 2015; Figure 3).

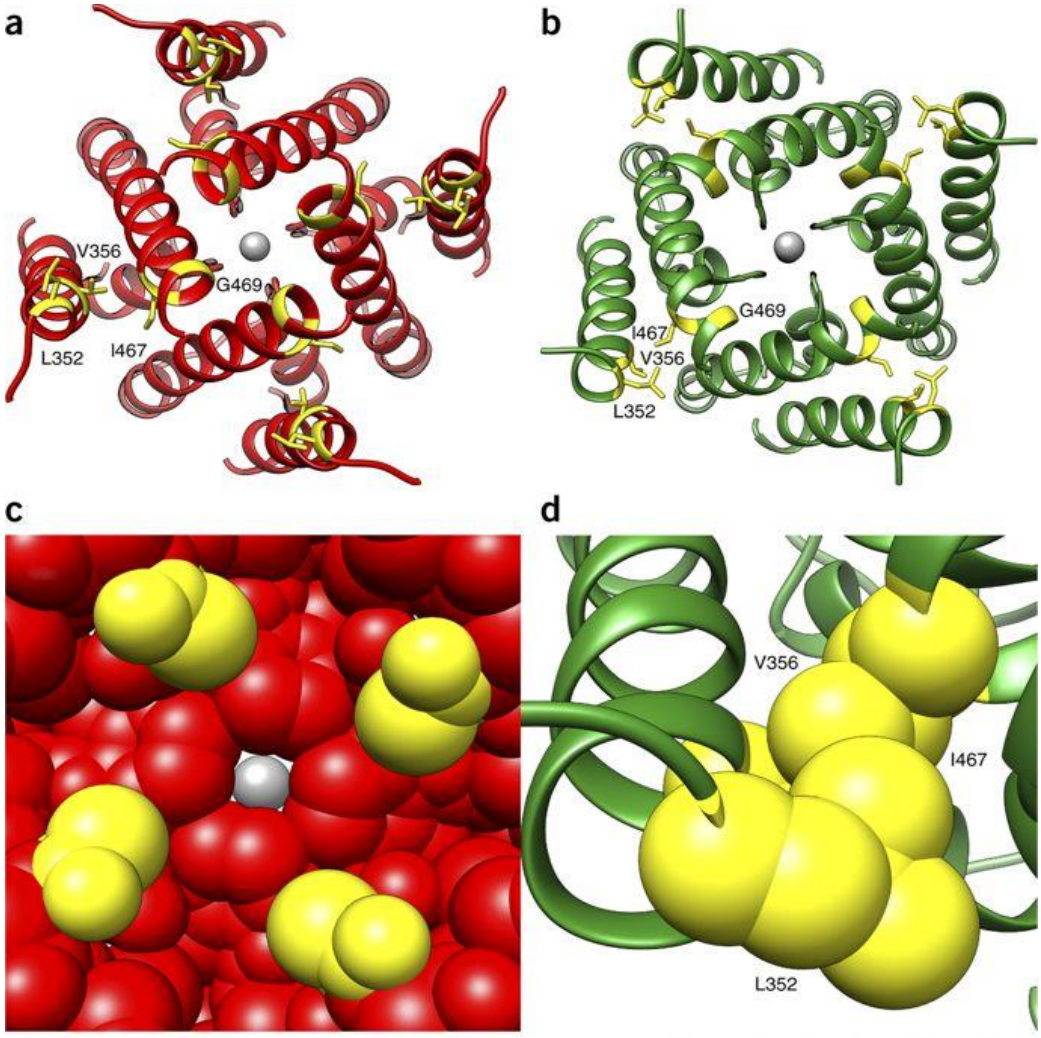

Figure 3. Structural impact of ZLS-associated KCNH1
Helices S5 and S6 of KCNH1 in their closed (A) and open (B) states are shown. The pore-closing region is enlarged in the closed state (C) and in the open state the hydrophobic cluster formed by Leu352, Val356 and Ile467 is enlarged (D), (Kortum et al. 2015).

The functional consequences of KCNH1 mutations identified in ZLS patients (p.Gly348Arg, p.Leu352Val, p.Ile467Val, p.Gly469Arg and p.Ser352Tyr/Val356Leu) were assessed by patch-clamp experiments on Chinese hamster ovary (CHO) cells expressing wild-type or mutant KCNH1 channels. An effect of gain of function for all disease-associated KCNH1 mutants was observed, showing a shift in the activation threshold to more negative potentials. The mutants channels exhibited accelerated channel activation

and slower deactivation, producing dramatic increases in whole cell K^+ conductance, compared to wild-type KCNH1 (Kortüm et al., 2015; Figure 4).

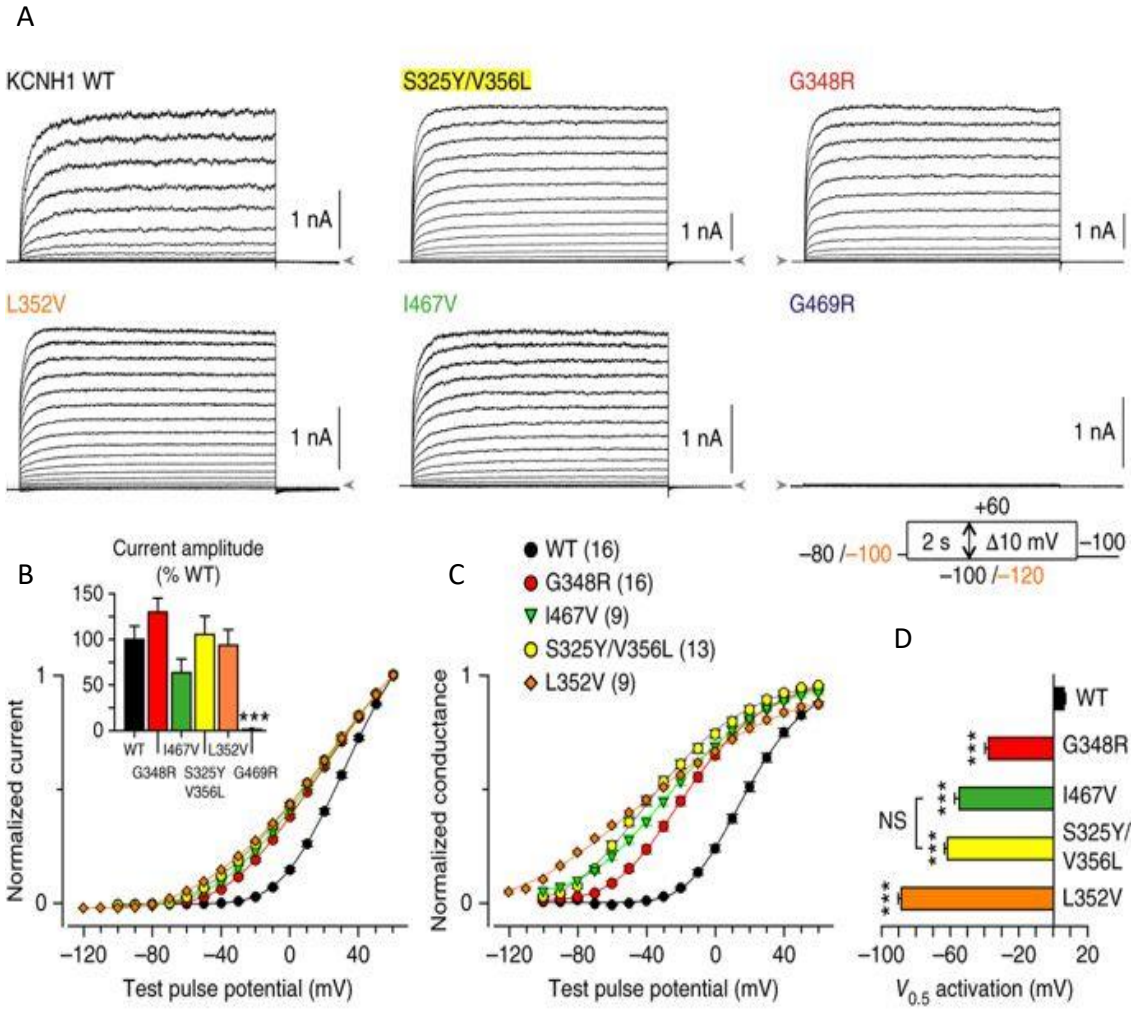

Figure4. Voltage-dependent activation of human wild-type (WT) and mutant KCNH1 channelsexpressed in CHO cells.

Families of whole-cell currents elicited with 2-s variable test pulses (A). KCNH1 current amplitudes as a function of the test pulse potential(B). Whole-cell conductance as a function of the test pulse potential (C). Potential of half-maximal KCNH1 channel activation ($V_{0.5\ activation}$), (Kortum et al. 2015) (D).

Simons et al. studied the effect of TMBTS associated-KCNH1 mutations (p.Ile467Val, p.Gln476Arg, p.Leu462Phe and p. Lys217Asn) in Xenopus oocytes and human HEK293T cells expressing mutant human channels and analyzed their activities using two-electrode voltage-clamp or patch-clamp electrophysiology. As for mutations in KCNH1 associated with ZLS, all TMBTS associated mutants showed enhanced activity and slower deactivation, compared to the wild-type channel (Simons et al., 2015; Figure 5).

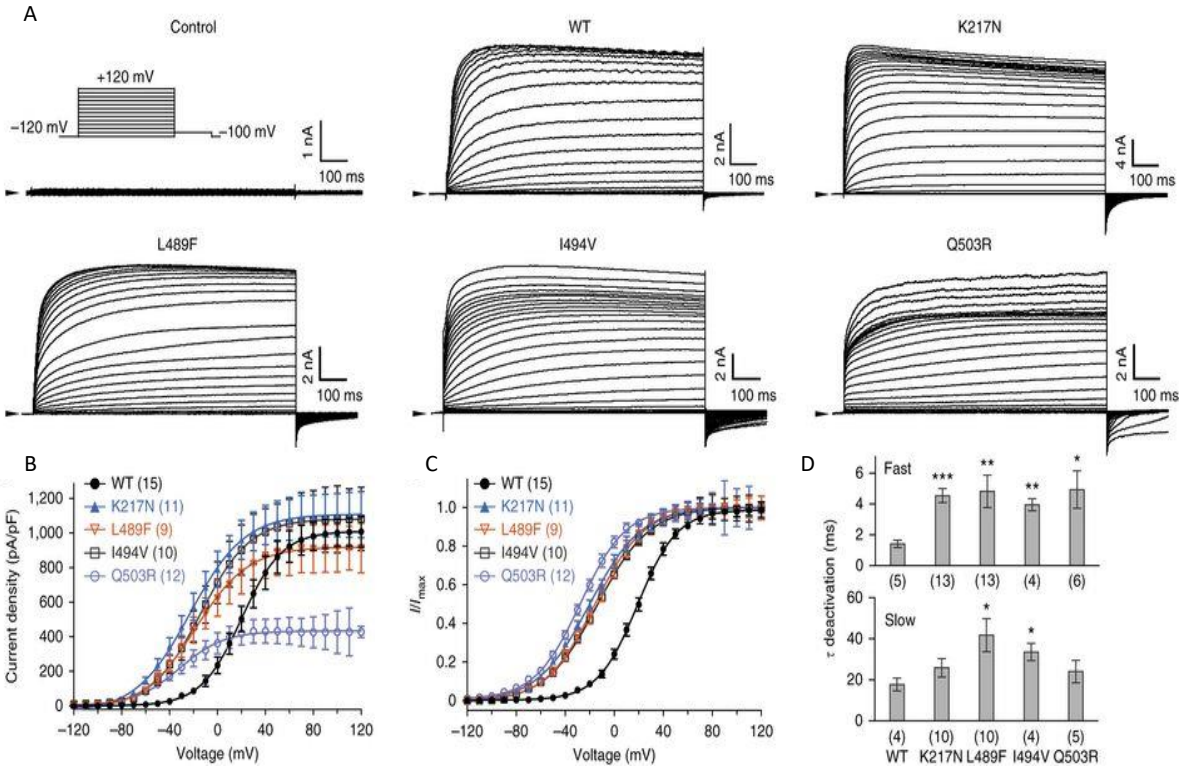

Figure 5. Mutant KCNH1 channels show a decreased activation threshold and delayed deactivation. (A) Whole-cell currents in HEK293T cells expressing wild-type (WT) and mutant KCNH1. (B) Current density versus test voltage for wild-type and TBS-associated mutant KCNH1 channels expressed in HEK293T cells. (C) Activation current-voltage relationship for wild-type, Lys217Asn, Leu489Phe, Ile494Val and Gln503Arg channels expressed in HEK293T cells. (D) Fast and slow time constants (τ) of deactivation for wild-type and mutant KCNH1 channels expressed in HEK293T cells (Simons et al., 2015).

The identical mutations in the voltage-sensing domain of *KCNH1*(c.989G>A, p.Arg330Gln; Bramswig et al., 2015) was found in three individuals of a cohort of intellectual disability. Moreover, a fourth individual was identified with a previously TMBTS described mutation (Simons et al., 2015) in the channel pore domain (c.1384C>T, p.Leu462Phe; Bramswig et al., 2015).In addition, Fukai et al. identified two novel *KCNH1* (1406G>A, p.Gly469Glu and c.989G>C,p.Arg330Pro) and a previously reported (c.989G>A, p.Arg330Gln; Bramswig et al., 2015) mutations in patients with SHDDH. In at least five cases, the same mutation has been reported in association with different clinical diagnosis (e.g. c.1399A>F, p.Ile467Val associated with ZLS and TMBTS, Kortum et al. 2015; Simons et al., 2015)(Table 1).

Despite these identified KCNH1 mutated patients could not be assigned to the same syndrome, a comparison of them, allowed to disclose the presence of some shared clinical features, like intellectual disability, craniofacial dysmorphism, seizures and/or epilepsy, and hypoplastic nails.

Mutation (NM_002238.3) (NP_002229.1)	Mutation (NM_172362.2) (NP_758872.1)	Diagnosis	n. of cases	Reference
c.651G>C p.K217N	c.651G>C p.K217N	TMBTS	1	Simons *et al.*2015
c.[974C>A;1066G>C] p.[S325Y;V356L]	c.[1055C>A;1147G>C] p.[S352Y;V383L]	ZLS	1	Kortum *et al.* 2015
c.989G>A p.R330Q	c.1070G>A p.R357Q	SID	3	Bramswig *et al.* 2015
		SDDHS	2	Fukai *et al.* 2016
		ZLS	1	Not published
c.989G>C p.R330P	c.1070G>C p.R357P	SDDHS	1	Fukai *et al.* 2016
c.1042G>A p.G348R	c.1123G>A p.G375R	ZLS	1	Kortum *et al*. 2015
		TMBTS	1	Mégarbané *et al.* 2016
		ZLS	1	*Mastrangelo et al.* 2016
c.1054C>G p.L352V	c.1135C>G p.L379V	ZLS	1	Kortum *et al*. 2015
c.1384C>T p.L462F	c.1465C>T p.L489F	TMBTS	1	Simons *et al.* 2015
		SID	1	Bramswig *et al.* 2015
c.1399A>G p.I467V	c.1480A>G p.I494V	ZLS	2	Kortum *et al.* 2015
		TMBTS	3	Simons *et al.* 2015
c.1406G>A p.G469E	c.1487G>A p.G496E	SDDHS	1	Fukai *et al.* 2016
c.1405G>A p.G469R	c.1486G>A p.G496R	ZLS	1	Kortum *et al*. 2015
c.1427A>G p.Q476R	c.1508A>G p.Q503R	TMBTS	1	Simons *et al.* 2015

Table 1. A summary of mutations identified in KCNH1 patients.
TMBTS= Temple–Baraitser Syndrome; ZLS= Zimmermann-Laband syndrome; SID= Syndromic Intellectual Disability; delay; SDDHD= Syndromic Developmental Delay Hypotonia and Seizures.

Epilepsy is a key manifestation in KCNH1-associated disorders but the mechanism by which *KCNH1* mutations cause epilepsy remains to be elucidated. A possible mechanism could be that gain of channel function results in increased K^+ conductance with subsequent inhibition of Na^+ and Ca^{2+} currents, two major effectors during epilepsy, and perturbation of neurotransmitter release. However, there is not a clear relationship among *KCNH1* mutations and severity, age of onset, response to antiepileptic drugs and type of seizures, that include focal motor seizures and generalized tonic-clonic seizures with seizure control (Mastrangelo et al., 2016).

1.2.2 Potassium channel subfamily K member 4 - *KCNK4*

KCNK4 (OMIM 605720), also known as TRAAK (TWIK-related arachidonic acid-stimulated K^+ channel), is one of three lipids and mechano-sensitive K2P channels constituting the TREK subfamily. Two-pore-domain (K2P) K^+ channels are dimeric proteins with a unique structure of four transmembrane domains and two pore-forming domains. The 15 mammalian members have been grouped into six subfamilies on

the bases of function and structure (Figure 6). In addition to physical factors such as pH, temperature and membrane stretch, K2P channels are regulated by neurotransmitters acting through G protein-coupled receptors, hormone, polyunsaturated fatty acids and by several medicinal agents, including volatile anaesthetics and respiratory stimulants, anti-psychotics, anti-depressants and neuroprotective agents (Noël et al., 2011).

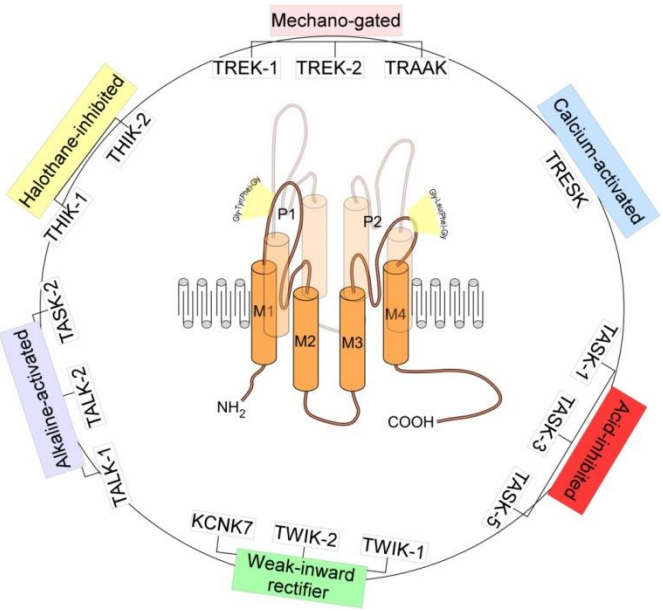

Figure 6. Structure and classification of K2P channels.
K2P channels are two-pore domain potassium channels and assemble as dimers of four transmembrane segments (M1–M4) and two-pore domain (P1 and P2). They have an extended M1-P1 extracellular loop and cytosolic N- and C-termini and a unique pore signature sequence Gly-Tyr(Phe)-Gly in the 1st pore (P1) and Gly-Leu(Phe)-Gly in the 2nd pore (P2)（Djillani et al., 2019).

KCNK4 gene is located on the long arm of chromosome 11 (11q13.1) and encodes for a 393 amino-acid long protein (NM_001317090.1, NP_001304019). KCNK4 is mainly expressed in the human and the rodent brains where it contributes to the background K^+ currents and regulate cell viability. In the mouse brain, KCNK4 mRNA is expressed in the whole hippocampus neurons. Moreover, it can be found in the spinal cord and retina (Fink et al., 1998).

Most studies on KCNK4 have focused on the functions and mechanism of the channel, such as its roles in CNS degenerative disease processes, synaptic transmission, the maintenance of membrane resting potential and cell volume regulation. In degenerative processes of ischemia-induced neurons, KCNK4 channel demonstrates the capability to downregulate neuronal excitability that leads to lower cellular metabolic rate (Noël et al., 2011).

All members of the TREK channel family, including KCNK4, are expressed in human retinal pigmented epithelial cells (RPE-1) and their activation protect cells against oxidative stress, which is important in the onset and development of retinal degeneration diseases. They increase the survival rates by enhancing the levels of intracellular protective factors, such as Bcl-2 and αB-crystallin and decrease

apoptosis by enhancing factors, such as Bax and cleaved-caspase-3. Moreover, under oxidative stress these channels protect the integrity of the RPE cell structure (Huang et al., 2018). However, the specific function of each member of these channels in regulating apoptosis and oxidative stress has not yet been characterized.

It is known that actin cytoskeleton inhibits mechanosensation of another member of TREK subfamily, KCNK2, and that this channel influences the assembly of the actin network and the formation of filopodia-like structures independently of its channel activity. However, the molecular mechanism of the cross-talk between the channel and actin is still unknown as well as the potential involvement of the other members of the family in modulating cytoskeletal structures like primary cilium (Noël et al., 2011).

K2P channels are dimeric proteins, with each subunit contributing two pore domains to the channel. Two different de novo missense mutations in *KCNK4* (c.515C>A, p.Ala172Glu and c.730G>C ,p.Ala244Pro), have been reported in three subjects (FHEIG syndrome, MIM 618381), highlighting the role of K^+ channels in developmental processes (Bauer et al., 2018). Subjects with FHEIG syndrome had significant generalized hypertrichosis and a similar facial gestalt, including hypotonic faces, bitemporal narrowing, micrognathia, deep-set eyes, bushy eyebrows and long eyelashes, low-set ears, short deep philtrum, gingival overgrowth, prominent upper and lower vermilion, and everted upper lip. Other more variable features included nystagmus with optic hypoplasia, hypotonia, hyperreflexia and DD/ID. Two of three patients showed also early-onset focal and generalized seizures (Bauer et al., 2018).

KCNK4 channel is a dimeric protein. Each subunit comprises an extracellular cap covering the pore, four transmembrane helices (M1 to M4) and two pore domains (P1 and P2) constituting the selectivity filter. Missense pathogenic mutations in KCNK4 mapped in regions of the channel possibly involved in KCNK4 activation: Ala244 is located at the center of helix M4 while Ala172 is located in M3 helix which interacts with M2 (Figure 7A). Channel opening is mediated by the transition of M4 helix: when the M4 helix is in the down state, lipid moieties insert in the lateral fenestration blocking K^+ flux; when the M4 is in the up conformation state, fenestration are closed, lipid insertion is prevented and the channel is open (Figure 7B). Molecular dynamics stimulations showed that M4 helixes of wild-type and of p.Ala172Glu mutant were in down state in absence of activating stimuli, in contrast to up conformation of M4 helixes of p. Ala244Pro mutant channel. Moreover, the lateral fenestration of both mutants were less open compared to wild-type, suggesting basal activation in mutants. p.Ala172Glu substitution induced the formation of an inter-domain salt bridge between Glu172 and Arg147 (helix M2) which might be responsible for the closing of fenestration, observed even though both helices were in down conformation (Figure 7C).

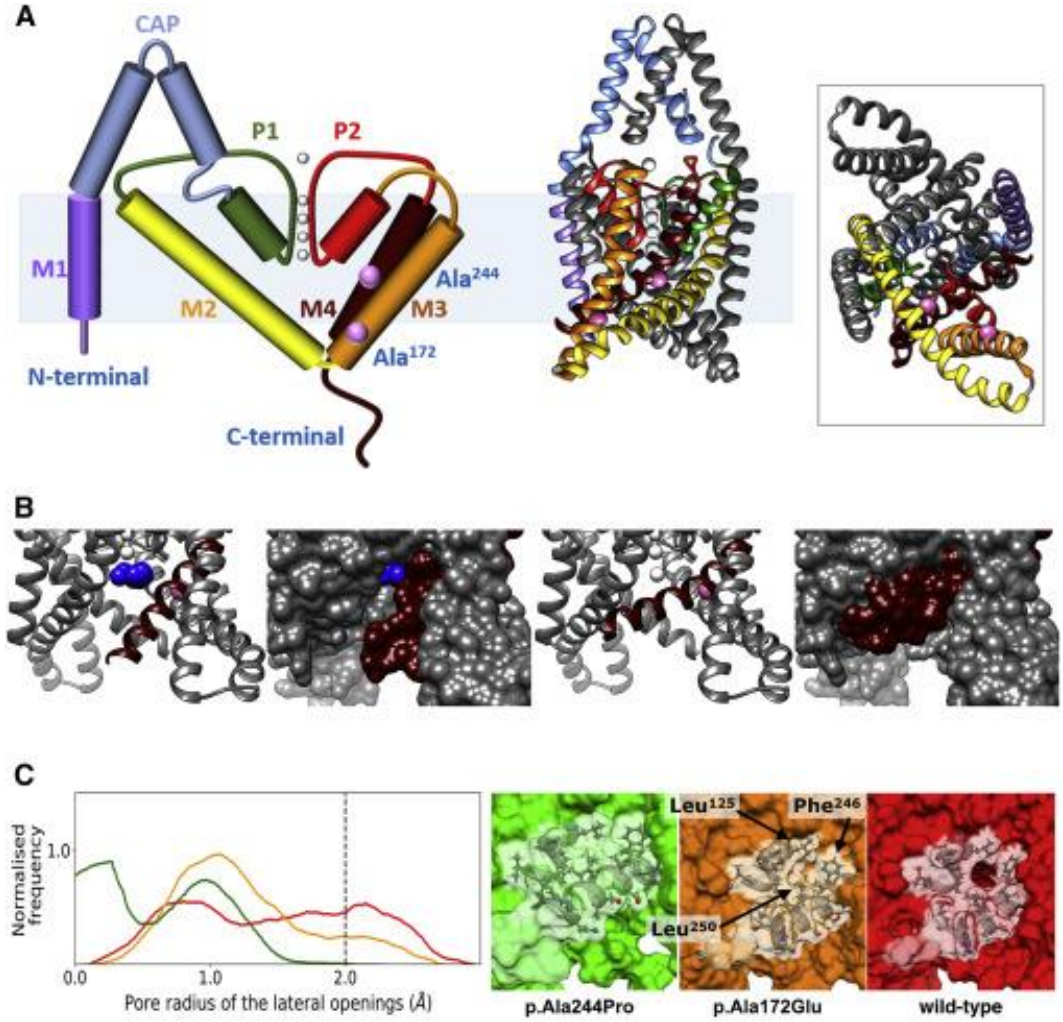

Figure 7. The schematic structure of KCNK4 monomer and location and structural consequences of disease causing mutations

(A) Schematic and crystallographic structure of KCNK4 channel. Each subunit of homodimer comprises an extracellular cap covering the pore, four transmembrane helices (M1 to M4), and two pore domains (P1 and P2) constituting the selectivity filter. (B) Structure of the KCNK4 channel in the two conformational states with open and closed lateral fenestrations. (C) Structural impact of the p.Ala244Pro and p.Ala172Glu amino acid substitutions, as observed in the molecular dynamics simulations. Residues Leu125, Phe246, and Leu250 involved in the hydrophobic cluster occluding the fenestration (Bauer et al., 2018).

Patch-clamp experiments were performed in order to explore the structural impact of p.Ala172Glu and p.Ala244Pro mutationsin transfected CHO cells (Figure 8). Both disease-associated amino acid substitutions have shown activating effect. The mutant channels p.Ala244Pro and p.Ala172Glu showed a higher maximal basal activity compared to the wild-type and could not be stimulated further by mechanical stimuli. In addition to their mechanosensitivity, KCNK4 is activated by arachidonic acid and polyunsaturated fatty acids. Both KCNK4 mutants were found to lack the channel activation in response to arachidonic acid, which likely reflects their basal maximal activation. Accordingly, the two disease-causing *KCNK4* mutations resulted in again of function effect, indicated by a dramatically increased basal K^+ conductance (Bauer et al., 2018).

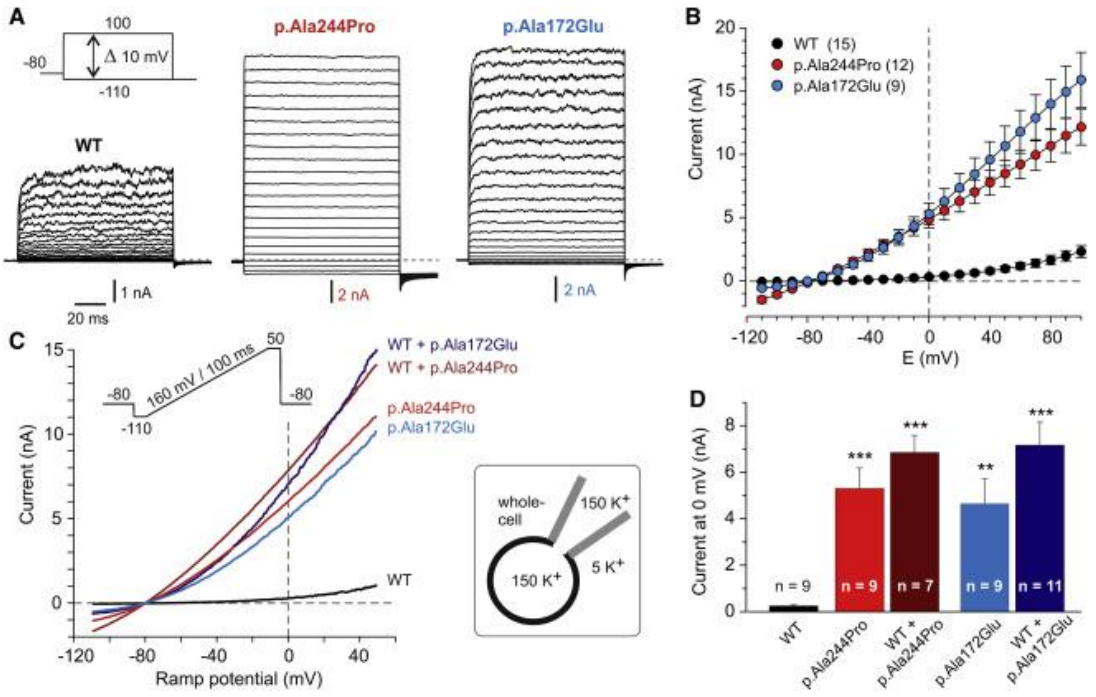

Figure 8. Whole-cell current recordings from CHO cells expressing wild-type or mutant KCNK4 channels

(A) Current recordings in cells expressing the wild-type (WT) or mutant (p.Ala244Pro or p.Ala172Glu) KCNK4 channels. (B) The I/V-plot shows current amplitudes recorded with the voltage step protocol. (C) I/V-plots of representative KCNK4 current recordings elicited with the ramp protocol shown as inset. Cells were previously transfected or co-transfected with cDNA coding for WT and mutant KCNK4. (D) Current amplitude at 0 mV ramp potential (Bauer et al., 2018).

Recently, dominantly acting missense mutations in *KCNN3*, coding for one of three members of the small-conductance Ca^{2+}-activated K channels (SK channels), were identified in three subjects with the major clinical features of ZLS and significant clinical overlap with KCNH1 ZLS- and KCNK4 FHEIG -related disorders (Bauer et al., 2019). With the identification of gain-of-function mutations in *KCNN3*, it has been proposed to include the phenotypes associated with mutations in *KCNH1*, *KCNK4*, and *KCNN3* in a new subgroup of neurological potassium channelopathies, characterized by developmental delay/ intellectual disability (DD/ID), coarse facial features, and gingival hyperplasia as common findings and epilepsy, hypertrichosis, and nail aplasia or hypoplasia as variable manifestations, associated with an increase in K^+ conductance, especially evident at negative membrane potentials (Bauer et al., 2019).

2. AIM OF THE WORK

Aberrant functionof K^+ channels have recently been documented to affect development and underlie syndromic disorders, including ZLS and FHEIG syndrome (Bauer et al., 2018).

The aims of this project were to gain insight on the specific cell functions of KCNH1 and KCNK4 channels and explore the functional impact of pathogenic KCNH1-ZLS and KCNK4-FHEIG mutations using cell models. To this aims, we obtained primary skin fibroblasts from ZLS and FHEIG patients, to be analyzed through molecular and cellular approaches.

Overall, our study contributed to highlight ion channel-independent function of KCNH1 and KCNK4 converging on some share cellular pathways whose alteration might affect development processes. Our understanding of the intracellular role of K^+ channels could contribute to shed light on the mechanisms of pathogenesis of ZLS related developmental processes.

3. MATERIALS AND METHODS

3.1 Cell Culture

Functional characterization of KCNH1 and KCNK4 wild-type and mutant proteins was carried out on Human Dermal Fibroblasts (HDF) obtained from ATCC and cultured skin fibroblasts obtained from subcutaneous biopsies of ZLS and FHEIG syndrome patients, as well as in human TERT-immortalized retinal pigment epithelial cell line (hTERT RPE-1) obtained from ATCC. We obtained primary skin fibroblasts of patients with *KCNH1* mutations causing ZLS (c.1054C>G, p.Leu352Val and c.989G>A, p.Arg330Gln; Kortüm et al., 2015) and with *KCNK4* mutations causing FHEIG syndrome (c.515C>A, p.Ala172Glu and c.730G>C ,p.Ala244Pro; Bauer et al., 2018). The p.Arg330Gln mutation in KCNH1 causing ZLS was also reported in two individuals with ID (Bramswig et al., 2015) and in three individuals with SDDHS (Fukai et al., 2016).

Fibroblasts and RPE1 cell lines were cultured in Dulbecco's modified Eagle's medium (DMEM)and in DMEM/F-12, respectively, both supplemented with 10% heat-inactivated fetal bovine serum (FBS, EuroClone) and 1% penicillin-streptomycin, at 37 °C with 5% CO_2.

3.2 Constructs preparation and mutagenesis

The human *KCNH1* coding sequence corresponding to the short isoform (NM_002238.3, NP_002229.1, 962 amino acids) was amplified from human fetal cDNA using the following primers: KCNH1 Forward 5'-GTTTCCTGCTGTCGTAAGAAGC-3'; KCNH1 Reverse 5'-TGTTGGTCATGTGGACATATGTG-3'. The PCR products were gel-purified using the Wizard SV Gel and PCR Clean-Up System kit (Promega) and cloned in pSC-A-amp/kan vector using the Strataclone TA Cloning Kit (Agilent) according to the manufacturer's protocol. Positive colonies were amplified, and plasmidic DNA purified with WizardPlus SV Minipreps DNA Purification Systemkit (Promega) was subjected to Sanger sequencing.

Then, the fragment corresponding to the KCNH1 isoform was cloned from pSC-A-amp/kan vector to the eukariotyc expression vector pCMV-TAG2A using the restriction enzymes sites BamHI and SalI. Missense mutations associated to ZLS (p.L352V; Kortüm et al., 2015) and ZLS, SID and SDDHS phenotypes (p.R330QBramswig et al., 2015; Fukai et al., 2016) were introduced by site-directed mutagenesis, using PickMutant Site-directed Mutagenesis kit (Canvax) in accordance with the manufacturer's protocol. All constructs were checked by direct sequencing.

3.3 Immunoelectron microscopy

hTERT RPE-1 cells were fixed in a mixture of 0.1% glutaraldehyde-2% paraformaldehyde, in 0.1 M phosphate buffer, pH 7.4, for 2 h at 25 °C, scraped, centrifuged, embedded into 10% gelatin (Sigma-Aldrich) in 0.1 M PBS, pH 7.4 and solidified on ice. After infusion in 2.3 M sucrose on at 4 °C, cell blocks

were mounted on aluminium pins and frozen in liquid nitrogen. Ultrathin cryosections (60 nm) were cut at -120°C using an Ultracut EM FC6 cryo ultramicrotome (Leica Microsystems), collected with 1% methylcellulose in 1.15 M sucrose in carbon coated grids and single- or double-immunolabelled with primary antibodies. Bound antibodies were visualized using goat anti-rabbit or anti-mouse antibodies conjugated with 10- or 15-nm colloidal gold (British BioCell International). Immunolabeling was performed with the primary polyclonal antibodies (KCNH1), grids were finally stained with 2% methylcellulose -0.4% uranyl acetate and analysed by a Philips CM10 and/or Morgagni transmission electron microscope.

3.4 Sub-cellular localization

For immunofluorescence analysis, $10x10^3$ of wild-type and mutated KCNH1 (p.Leu352Val and p.Arg330Gln;) and KCNK4 (p.Ala172Glu and p.Ala244Pro) fibroblasts and $25x10^3$ of hTERT RPE-1cell lines were seeded in 24-well cluster plates onto 12-mm cover glasses and maintained in culture complete medium for 48h. hTERT RPE-1 cells were transfected with vectors expressing wild-type or mutants Flag-tagged KCNH1, respectively, using Lipofectamine 3000. After 48h of transfection (for hTERT RPE-1) or culture (for fibroblasts) cells were fixed with 4% paraformaldehyde (20 min at RT). After permeabilization with 0.1% Triton X-100 (10 min at room temperature), non-transfected cells were stained with selected primary antibodies anti-KCNH1 (sigma) and KCNK4 (Sigma), whereas transfected hTERT RPE-1 were stained with anti-Flag (SIGMA). To investigate the specific sub-cellular localization of the two K^+ channels, co-localization analysis was performed using specific cellular organelles markers: Golgin (Sigma) for the Golgi apparatus, RAB5 (Santa Cruz Biotecnology) for early endosomes, acetylated α-Tubulin (Santa Cruz Biotecnology) for primary cilium assoneme, CEP170 and CEP164 (Santa Cruz Biotecnology) for cilium basal body, EHD (Santa Cruz Biotecnology) for ciliary pocket, Lamin A/C (Sigma) for nuclear membrane, Fibrillarin (Santa Cruz Biotecnology) for nucleolus, and Ki-67 (Santa Cruz Biotecnology) for nucleus. The appropriate secondary antibodies were used (Invitrogen) followed by nuclei staining with Dapi (Sigma). Coverslips were extensively rinsed and mounted onto microscope slides using mounting medium (Sigma). 3D images were sequentially acquired by Olympus' PLAPON60XOSC2 super-corrected objective confocal apparatus.

3.5 Cilia formation and Immunofluorescence

To explore the role of KCNH1 mutations in cilium assembly/disassembly, dynamics immunofluorescence analyses were performed. To this aim, HDF and hTERT RPE-1 cells were plated onto coverslips and cultured in complete medium for 24h. The day after, cells were serum starved in serum free media to induce ciliogenesis and after 48h serum was reintroduced for 1, 2 and 4h to induce cilia disassembly. At the end of incubation period, cells were washed with Phosphate Buffered Saline (PBS), fixed using 4% paraformaldeyde and permeabilized with 0.1% Triton X-100. Primary cilia were

visualized by acetylated α-tubulin (Santa Cruz Biotecnology, axoneme), Arl13b (Proteintech, axoneme), IFT172 (Santa Cruz Biotecnology, anterograde transport) and CEP170 and CEP164 (Santa Cruz Biotecnology, basal body) staining. Images were captured by confocal microscopy on Olympus FV1000.

For quantification of primary cilia, both acetylated α-tubulin and CEP170 labelling were used to define cilia. The proportion of ciliated cells in a given field was determined by counting the number of cilia and the number of nuclei present and was expressed as percentage of total cell population. Cilium prevalence was measured for 6 fields in three separate experiments. Sequential 0.5 µm thick z-stacked sections were imaged through the entire cell profile using a 60X objective lens and were used to create maximum intensity projections (MIPs). ImageJ analysis software was used to measure the morphology of cilia and the co-localization in MIPs. Statistical significance was determined by unpaired t-test.

3.6 Fibroblasts growth curve

Once the fibroblasts reached 80 to 90% of confluence, they were plated at a density of $1x10^4$ cells per well in a 24 well plate and incubated at 37°C/5% CO_2 on DMEM with 10% fetal bovine serum, for 24, 48, 72 and 96 hours. A combination of Trypsin/Ethylene Diamine Tetra Acetic acid (EDTA) solution was used to detach cells from tissue culture dishes, and detachment was monitored by means of light microscopy. Trypsin/EDTA action was neutralized with media containing 10% FBS. The density of cells was assessed by counting cells in a Burker chamber. The cell concentration and growth rate were recorded in triplicate at defined time points (0, 24, 48, 72 and 96 h after plating).

3.7 Protein extraction, SDS-PAGE and western blotting

For western blot analyses, cell pellets were washed twice in PBS and lysed in RIPA buffer (20 min, 4 °C). with 1 × Protease and Phosphatase Inhibitor Cocktail. Lysates were kept for 30 min on ice and then centrifuged for 10 min at 14 000 × g at 4 °C. Supernatants were collected and assayed for protein quantification by the Bradford method (Serva). Analysis of protein components was performed by polyacrylamide gel electrophoresis separation (Bio-Rad) and transferred onto nitrocellulose membranes (Amersham Biosciences). After saturation, blots were incubated overnight at 4 °C, with anti-Bcl2 (Santa Cruz Biotecnology) antibody, and finally incubated for 1 h with HRP-conjugated secondary antibodies and detected on X-ray film (Aurogene) using the ECL Advance Western Blotting Detection Kit (Amersham Biosciences). Quantifications were performed by ChemiDoc (Biorad). GAPDH (Sigma) was used for protein normalization. Densitometric analyses were performed with the ImageJ software.

3.8 Real-Time Quantitative PCR

Total RNA was extracted from wild-type and mutated KCNH1 (p.Leu352Val and p.Arg330Gln) and KCNK4 (p.Ala172Glu and p.Ala244Pro) fibroblasts with TRIzol Reagent(Invitrogen) according to the manufacturer's instructions. Briefly, fibroblasts were homogenized in TRIzol and chloroform was added

at 1:5 of the initial volume of TRIzol. Sample were incubated at room temperature for 15 min and then centrifugated at 12,000 × g for 15 min at 4 ° C. After centrifugation, aqueous phase was transferred to a new tube, mixed with 0.5 ml of cold isopropyl alcohol, placed at 4 ° C for 20 min, and then centrifuged at 12,000 × g for 10 min at 4 ° C. The RNA pellet was washed with 75% ethanol, dried by air, and dissolved in 0.01% diethyl pyrocarbonate water. The purity and amounts of the RNA obtained were checked by measuring optical density at 260 and 280 nm with the Nanodrop 100 System (Rockford, IL). A total amount of 1ug RNA was reverse transcribed using random primers with the High Capacity cDNA Reverse Transcription Kit (Applied Biosystem), according to the manufacturer's instructions. QPCR for *PTCH1*, *BCL2* and *SMO* genes quantification was performed using SYBR Green select (Applied Biosystems). Relative gene expression was calculated by ΔΔCt analysis, relative to *GAPDH* expression levels.

Primers were as follows:

BCL2 Forward 5' CGGAGGCTGGGATGCCTTTG 3'
BCL2 Reverse: 5' GTGATGCAAGCTCCCACCAG 3'

PTCH1Forward 5' CAACTCAGGTTTTGCCATTTC 3'
PTCH1 Reverse 5' CCGGTCCTGTCCTCAAAAG 3'

SMO Forward: 5' CTCATCCGAGGAGTCATGAC 3'
SMO Reverse 5' CAAAAATGCCCAGGCGCAGC 3'

GAPDH Forward5' TCTTTTGCGTCGCCAGCCGAG 3'
GAPDH Reverse 5' TGACCAGGCGCCCAATACGAC 3'

4. RESULTS

4.1 Characterization of the effect of KCNH1 and KCNK4 mutations on cell cycle

Proliferation is one aspects of cell physiology where K^+ channels play a crucial role and it is known that KCNH1 plays an active role in cell cycle progression in both cancer and non-transformed cells (Urrego et al., 2014). To investigate if mutations in KCNH1 and KCNK4 channels affect fibroblasts cell cycle we assayed cell proliferation by counting cell number as a function of time, using human dermal fibroblasts (HDF) as a control. We obtained primary skin fibroblasts of patients with KCNH1 mutations causing ZLS (p.Leu352Val and p.Arg330Gln; Kortüm et al., 2015) and with KCNK4 mutations causing FHEIG syndrome (p.Ala244Pro and p.Ala172Glu; Bauer et al., 2018). When grown in the same culture conditions, KCNH1 p.Leu352Val (Figure 9A) and KCNK4 p.Ala244Pro (Figure 9B) fibroblasts proliferated at a reduced rate compared to control fibroblasts (wild-type).

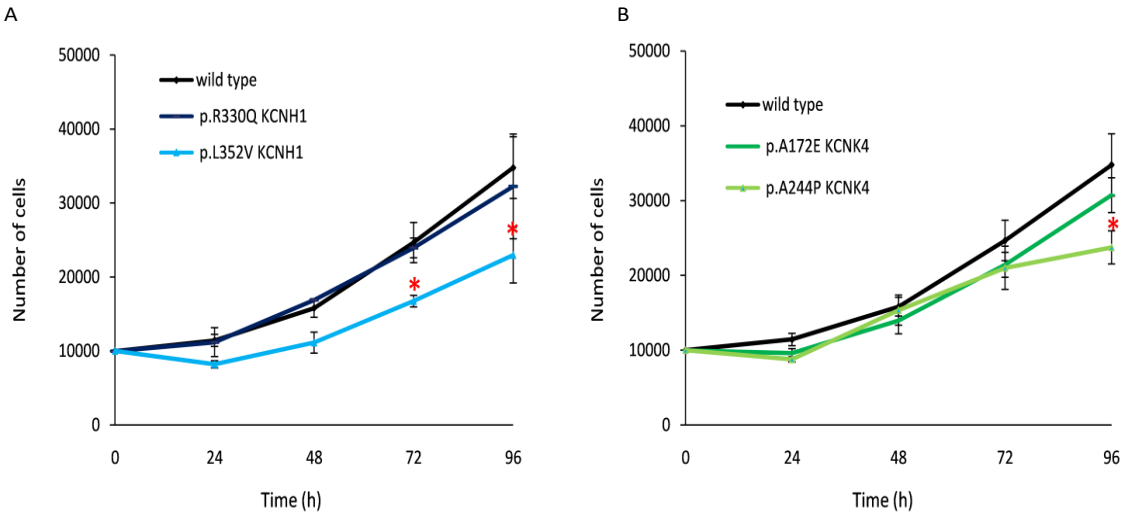

Figure 9. Mutations of *KCNH1* and *KCNK4* induce decreased cell proliferation.
The figure shows the growth curves of two ZLS (A), two FHEIG (B) patient's derived fibroblasts compared to wild-type fibroblasts. Cells were seeded for each sample and counted at the indicated time-points. *P≤0.05. Statistical significance was assessed using Student's t-test.

4.2 Characterization of the effect of KCNH1 and KCNK4 mutations on ciliogenesis

Ciliogenesis has been associated with cell cycle and control of cell proliferation (Malicki et al., 2017) therefore, as we disclosed an altered proliferation rate of mutated fibroblasts, we investigated a potential correlation between ciliation and the differential growth rate observed in ZLS and FHEIG fibroblasts. We measured ciliogenesis of mutant versus wild-type HDF using the serum starvation assay. Primary cilium was identified by immunofluorescence/confocal microscopy using antibodies against alpha acetylated-tubulin to label the microtubule axoneme in primary cilium, and CEP170 to label the basal body and the ciliated fractions in fibroblasts cultures. After 48h of serum starvation primary cilium was observed in most of cells

without any significant difference between wild-type and patients. Differently, before starvation there was a significant increase in the number of primary ciliated cells in cycling KCNH1 (p.Leu352Val and p.Arg330Gln) and in KCNK4 (p.Ala224Pro and p.Ala172Glu) patient-derived fibroblasts (Figure 10). Our data shows that all mutants studied display enhanced ability to promote cilia formation in cycling rather than in quiescent cells, compared to wild-type protein. Moreover, KCNH1 p.Leu352Val and KCNK4 p.Ala172Glu and p.Ala244Pro fibroblasts showed decreased ability to disassemble primary cilium after serum stimulation compared to wild-type fibroblasts.

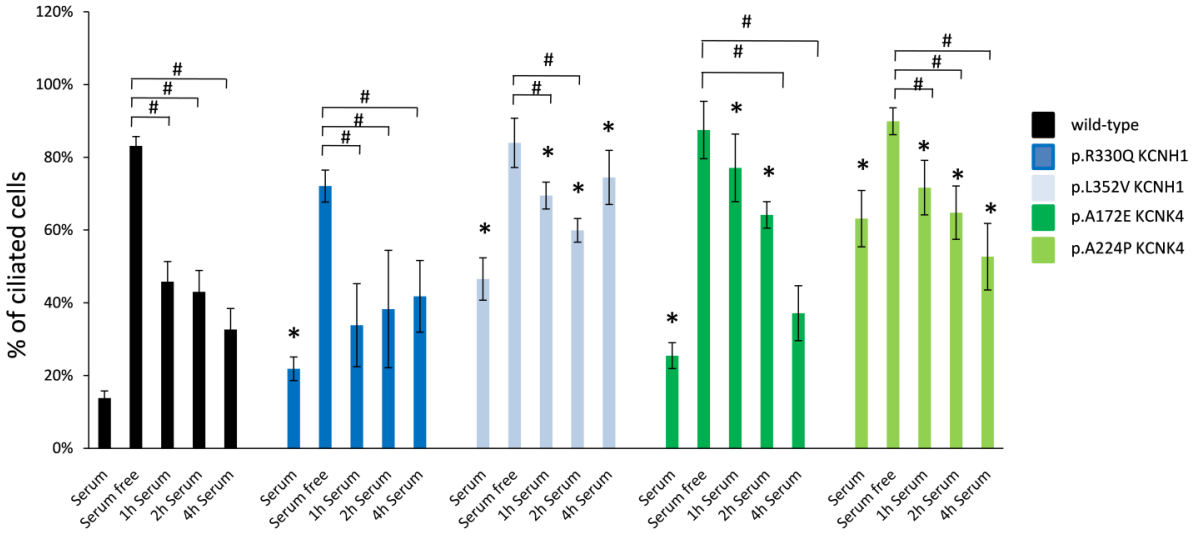

Figure 10. Mutations of KCNH1 and KCNK4 impair ciliogenesis.
Control and patient's fibroblasts were serum starved in serum free media to induce ciliogenesis and after 48h serum was reintroduced for 1, 2 and 4h to induce cilia disassembly. Percent of ciliated cells was counted using alpha acetylated tubulin/CEP170 as primary cilia markers. *P≤0.05 vs wild-type; #P≤0.05 vs serum free. Statistical significance was assessed using Student's t-test.

4.3 KCNH1 and KCNK4 variants affect SHH pathway

The primary cilium contains a highly specialised and compartmentalized molecular environment. For example, the Sonic hedgehog (SHH) signalling machinery is selectively localised to primary cilium structure.

In light of our previous results on cell proliferation and ciliogenesis, we sought to assess whether the SHH pathway was deregulated in the presence of mutant KCNH1 and KCNK4 proteins. We evaluated the basal expression levels of selected SHH target genes (*BCL2*, *PTCH1* and *SMO),* in HDF and mutant KCNH1 and KCNK4 patient's-derived fibroblasts, by quantitative real-time PCR. Interestingly, the basal expression levels of two key SHH-target genes, *BCL2* and *PTCH1,* were significantly higher in p.Arg330Gln KCNH1 mutated fibroblasts compared to control, whereas *SMO* gene appeared to be deregulated without reaching statistical significances (Figure 11A). A comparable trend of *PTCH1* and *SMO* transcripts expressions was observed in fibroblasts carrying p.Leu352Val mutation in KCNH1 (Figure 11A), which also showed a significantly over expression of BCL2 at the protein levels, as assessed by western blot analysis (Figure 11C).

Moreover, the basal transcript expression levels of both *BCL2*and *PTCH1* were significantly higher in p.Ala172Glu KCNK4 mutated fibroblasts compared to control (Figure 11B). BCL2 expression appeared to be deregulated in p.Ala244Pro KCNK4 mutated fibroblasts levels without reaching statistical significances both at the RNA (Figure 11B) and protein levels (Figure 11D). Our results demonstrated a significant dysregulation of the SHH signaling in KCNH1 and KCNK4 mutant cells compared to controls.

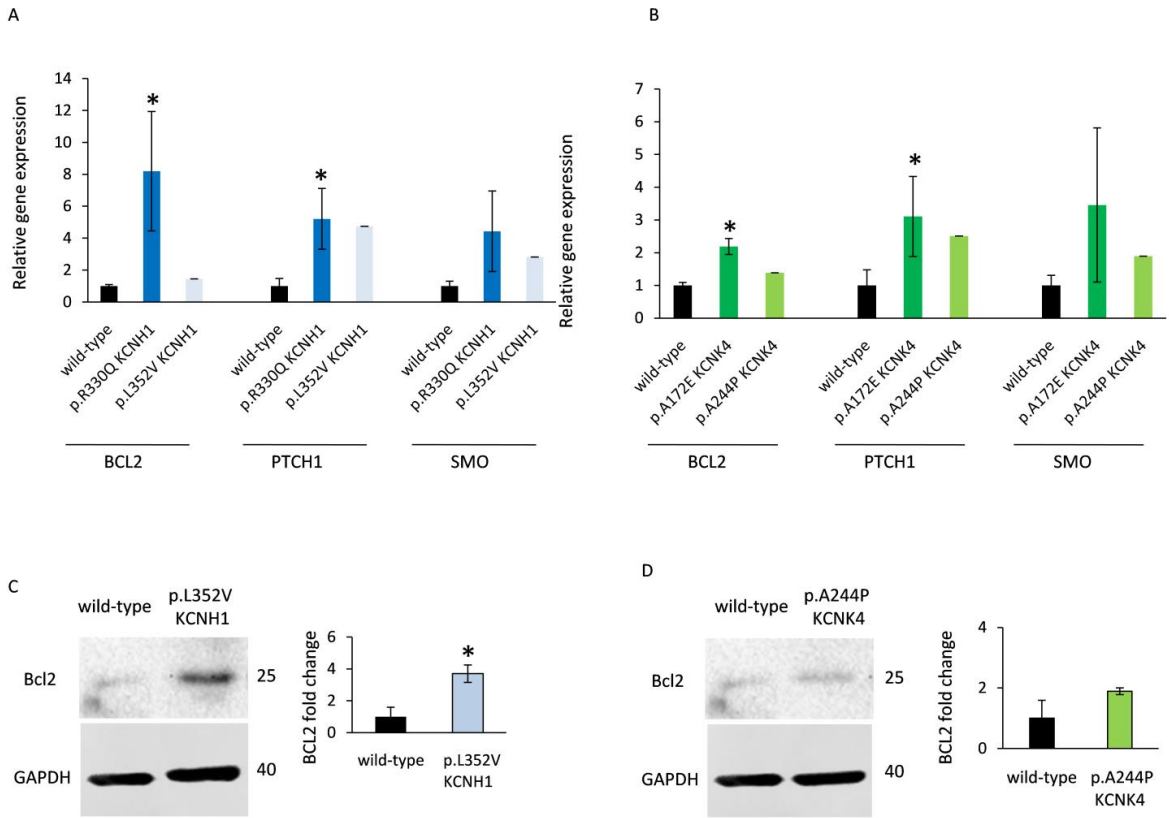

Figure 11. The SHH pathway is deregulated in KCNH1 and KCNK4 patient's fibroblasts.
RNA extracts from wild-type, KCNH1 and KCNK4 patient's fibroblasts were analyzed by RT-qPCR using specific primers for human *BCL2*, *PTCH1* and *SMO* genes using the ΔΔCt method (A, B). *P≤0.05. Statistical significance was assessed using Student's t-test. Proteins were extracted from wild-type, KCNH1 and KCNK4 patient's fibroblasts. Protein lysates were subjected to western blotting analysis with the specified antibodies. Representative western blotting images and statistical analysis of BCL2 protein expression. Western GAPDH antibody was used for normalizations (C, D). Normalized values are means ± S.E.M. *P≤0.05. Statistical significance was assessed using Student's t-test.

4.4 Characterization of the effect of KCNH1 mutations on KCNH1 sub-cellular localization

To evaluate whether the mutations in KCNH1 affect the sub-cellular localization of the channel, we performed immunofluorescence studies on primary skin fibroblasts of ZLS patients using specific sub-cellular compartments markers antibodies (Golgi apparatus and endosomes) and a commercially available KCNH1 antibody to stain KCNH1. Confocal laser-scanning microscopy analysis revealed cytoplasmic localization of KCNH1 with a reliable localization at the perinuclear and endosomal regions. In particular, as

shown in Figure 12A, KCNH1 showed partial overlap with the early endosome marker Rab5 in both wild-type and p.Arg330Gln mutated fibroblasts. On the contrary, we did not observe co-localization with Golgi marker (Figure 12B). A similar distribution was also observed in cells with the p.Leu352Val KCNH1 mutation.

Moreover, immunogold electron microscopy performed in hTERT RPE-1 cells revealed intracellular gold particles labeling KCNH1 in Golgi apparatus, endosomes and plasma membrane, consistently with immunofluorescence analyses (Figure 12C).

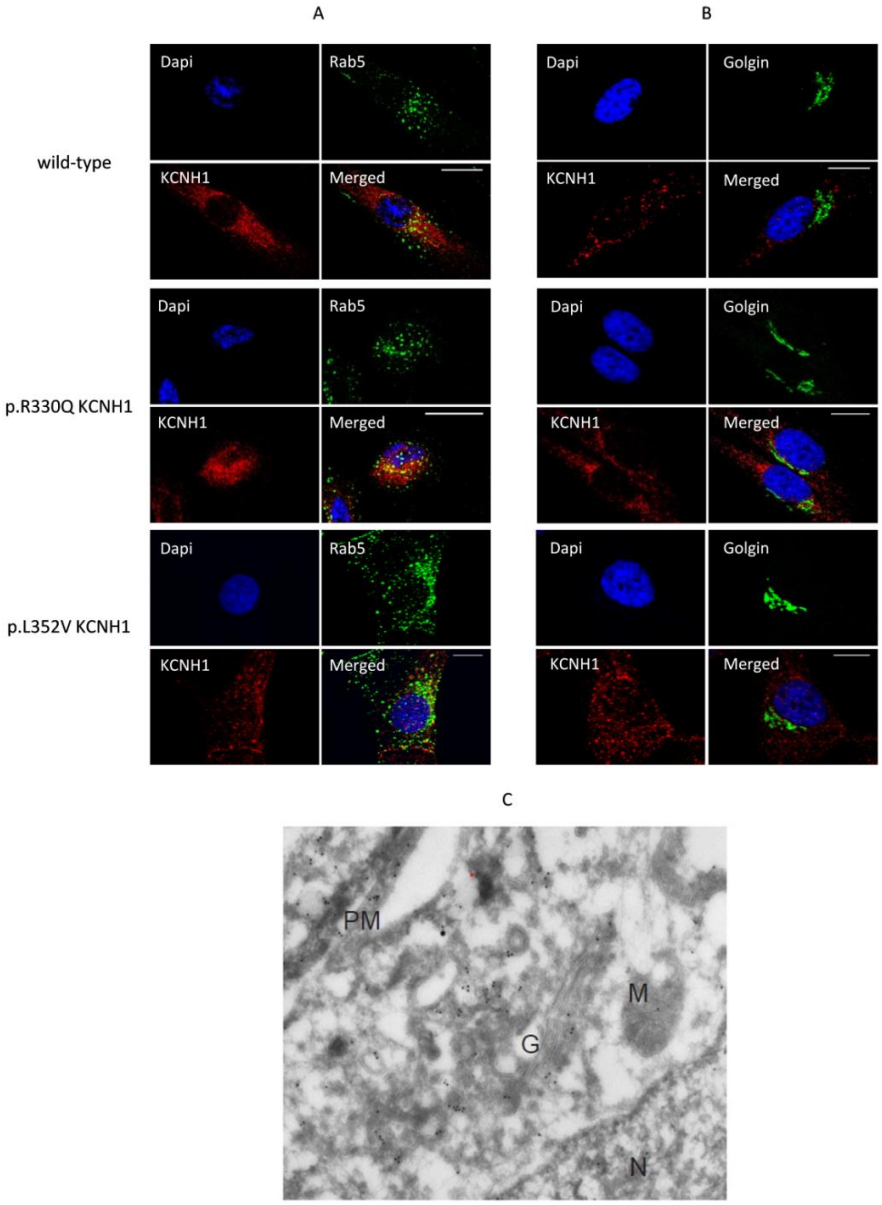

Figure 12. Co-localization of KCNH1 with endosome and Golgi markers in wild-type and patient's fibroblasts.

A. Wild-type and patient's fibroblasts were co-stained with anti-KCNH1 (red labelled) and anti Rab5 (green labelled). Nuclei (blue) were visualized by DAPI staining. Co-localization of KCNH1 and Rab5 is yellow (merged). Scale bar: 10 µm. B. Wild-type and patient's fibroblasts were co-stained with anti-KCNH1 (red labelled) and anti Golgin (green labelled). Nuclei (blue) were visualized by DAPI staining. No specific co-localization was observed between KCNH1 and Golgin. Scale bar: 10 µm. C. Immunoelectron microscopy of 48h serum starved hTERT RPE-1 cells shows intracellular localization of KCNH1. Gold particles are observed in the Plasma membrane, Golgi apparatus and endosomes.N = Nucleus, PM=Plasma Membrane, G= Golgi apparatus, M=Mitochondrion.

4.5 Characterization of the effects of KCNH1 mutations on protein localization

Preliminary recent work related KCNH1 with primary cilium in hTERT RPE-1 and in mouse embryonic fibroblasts (Sánchez et al., 2016). However, the specific KCNH1 cilium localization and function have not been characterized. In order to characterize the link between KCNH1 and primary cilium and to test if major pathogenic mechanisms of mutants KCNH1 relies on cilium localization, we performed immunofluorescence experiments in hTERT RPE-1 cells, in human control fibroblasts and primary skin fibroblasts derived from patients with two KCNH1 missense mutations causing ZLS (Kortüm et al., 2015). We used alpha acetylated tubulin, CEP164 and EHD as specific ciliary markers. Acetylated tubulin is a protein associated with axoneme assembly, CEP164 is a basal body protein required for assembly of the primary cilium and EHD proteins regulate endocytic events and localize to the ciliary pocket.

As shown in Figure 13, wild-type KCNH1-stained vesicular rosettes were near the outermost boundary of the centrosome defined by CEP164. In particular, KCNH1 showed partial overlap with the distal appendage marker CEP164 (Figure 13A) and the ciliary pocket marker EHD (Figure 13B), suggesting a localization of KCNH1 in the ciliary pocket. No difference in proteins' localization was observed between the wild-type and the p.Arg330Gln and p.Leu352Val missense mutants.

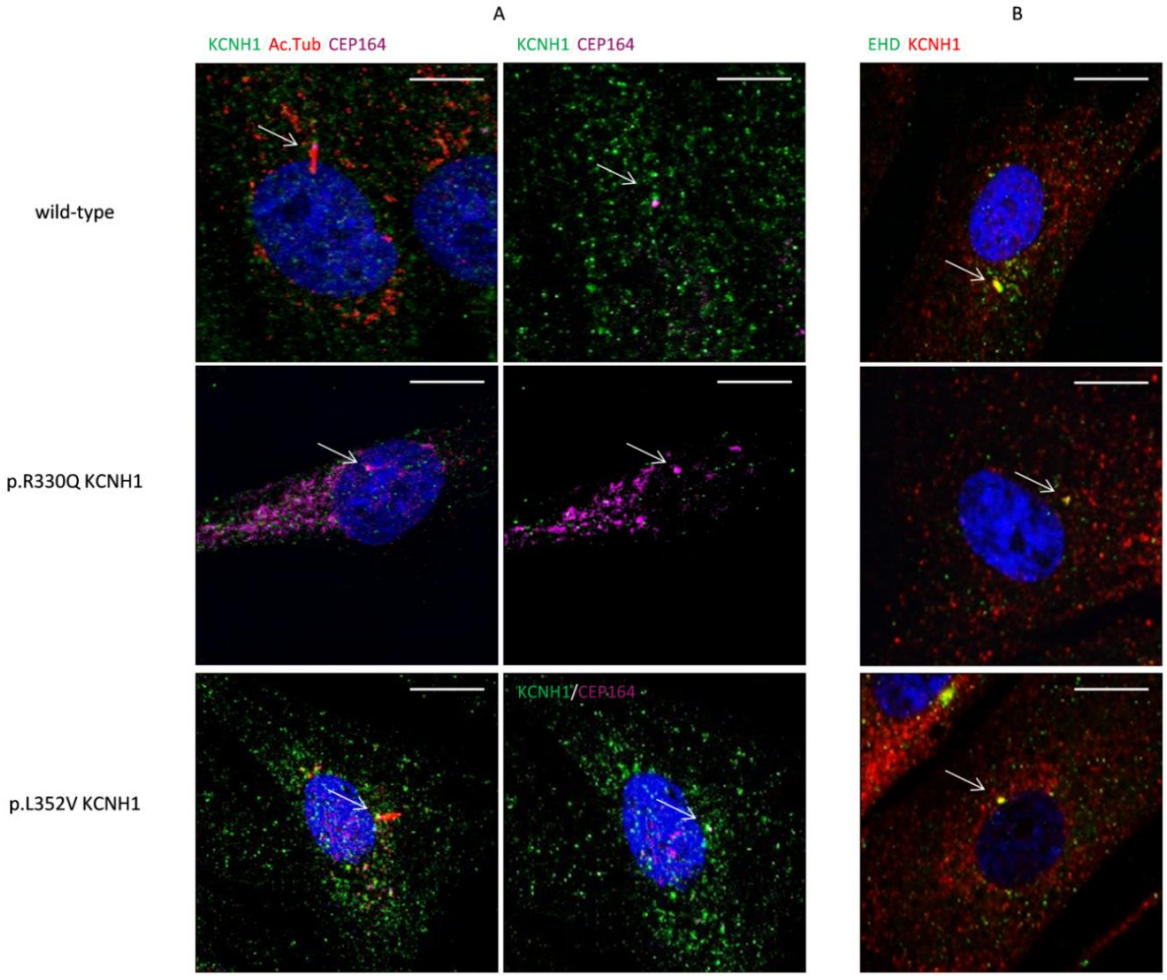

Figure 13. Localization of KCNH1 at the cilium base in wild-type and p.Arg330Gln and p.Leu352Val KCNH1- patients' fibroblasts.

A. Wild-type and patient's fibroblasts were starved for 48h prior to fixation and immunostaining procedures. Acetylated alpha tubulin (red) and CEP164 (pink) were used to mark the assoneme and the centrosome. Nuclei (blue) were visualized by DAPI staining. Zoomed-in areas in micrographs indicate localization of wild-type and mutant KCNH1 (green) proteins at the proximal end of the axoneme. Co-localization of KCNH1 and CEP164 is blank. Scale bar: 10 µm.B. Wild-type and patient's fibroblasts were starved for 48h prior to fixation and immunostaining procedures. EHD was used to mark the ciliary pocket and nuclei (blue) were visualized by DAPI staining. Co-localization of KCNH1 (red) and EHD (green) is yellow. Scale bar: 10 µm.

The same approaches were used on hTERTRPE-1 cells, transfected with C-terminal Flag-tagged KCNH1. According to the results obtained in fibroblasts, wild-typeKCNH1 localized near the base of primary cilia, as well as p.Leu352Val and p.Arg330Gln mutant proteins (Figure 14).

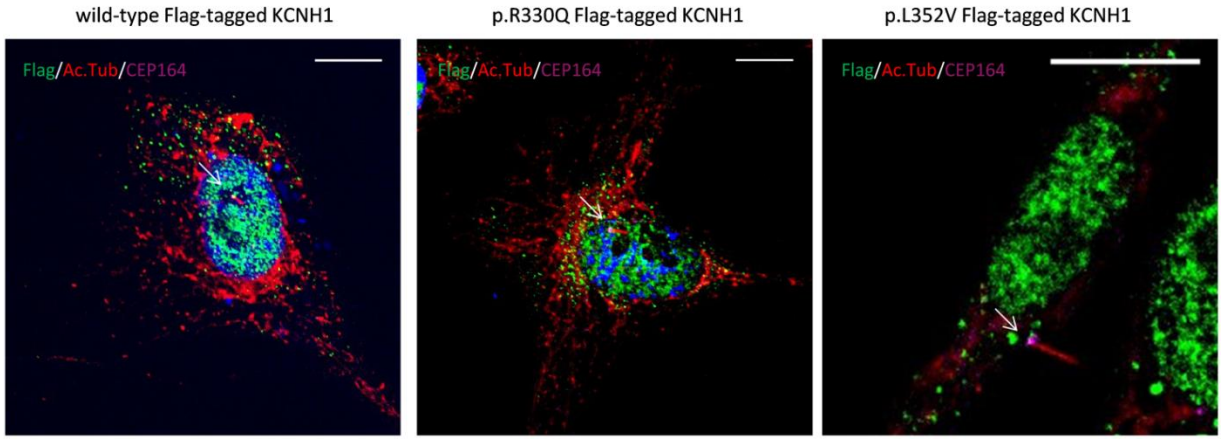

Figure 14. Exogenous Flag-tagged KCNH1 localizes to the primary cilia.
hTERT RPE-1 cells were transfected with plasmid expressing KCNH1 flag-tagged wild type, p.Arg330Gln and p.Leu352Val mutant proteins. The staining was performed using anti-flag (green), anti-acetylated alpha tubulin (red) and anti-CEP164 (pink) antibodies. The panel shows localization of KCNH1 to the primary cilium base (white arrow). Scale bar: 10µm.

4.6 Characterization of the effect of KCNH1 mutations on primary cilium morphology and function

We evaluated morphology of primary cilium in control and ZLS patient's fibroblasts. We characterized cilia morphology of 48h serum starved fibroblasts. A proportion of p.Arg330Gln fibroblasts showed a discontinuous axoneme, marked by a gap in Arl13b staining in all z-planes and bulbous tips (Figure 15A). Dysmorphic features were also observed in hTERT RPE-1 cell lines transfected with p.Arg330Gln Flag-tagged KCNH1 construct, which exhibited a bulbous projection at the tip (Figure 15B).

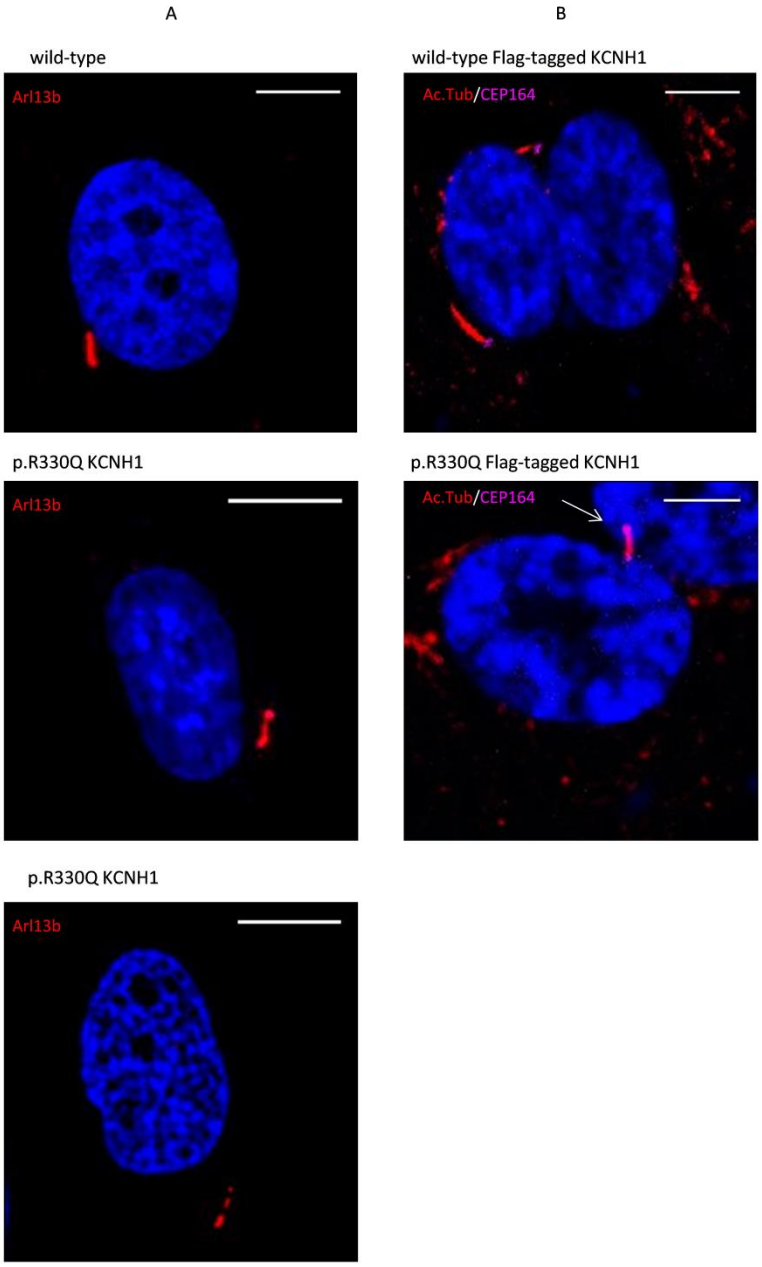

Figure 15. p.Arg330Gln KCNH1 mutation affects cilia morphology in quiescent cells.

A. Immunofluorescence microscopy of ciliated wild-type and p.Arg330Gln KCNH1 fibroblasts stained with antibodyto Arl13b (red). DNA was visualized with DAPI (blue). p.Arg330Gln fibroblasts show dysmorphic features (bulbous tip and discontinuous assoneme) compared to the control. Scale bar: 10 µm.

B. Immunofluorescence microscopy of ciliated hTERT RPE-1 cells transfected with plasmid expressing KCNH1 Flag tagged expressing wild-type and p.Arg330Gln mutant proteins. The staining was performing using anti-acetylated alpha tubulin (Ac.Tub, red) and CEP164 (pink) antibodies and DNA was visualized with DAPI (blue). p.Arg330Gln mutations leads to formation of bulbous ciliary tip. Scale bar: 10 µm.

In addition, structural abnormalities were detected in KCNH1 p.Leu352Val fibroblasts and hTERTRPE-1 cells transfected with p.Leu352Val Flag-tagged KCNH1, in which a portion of cells shows multiple cilia (Figure 16).

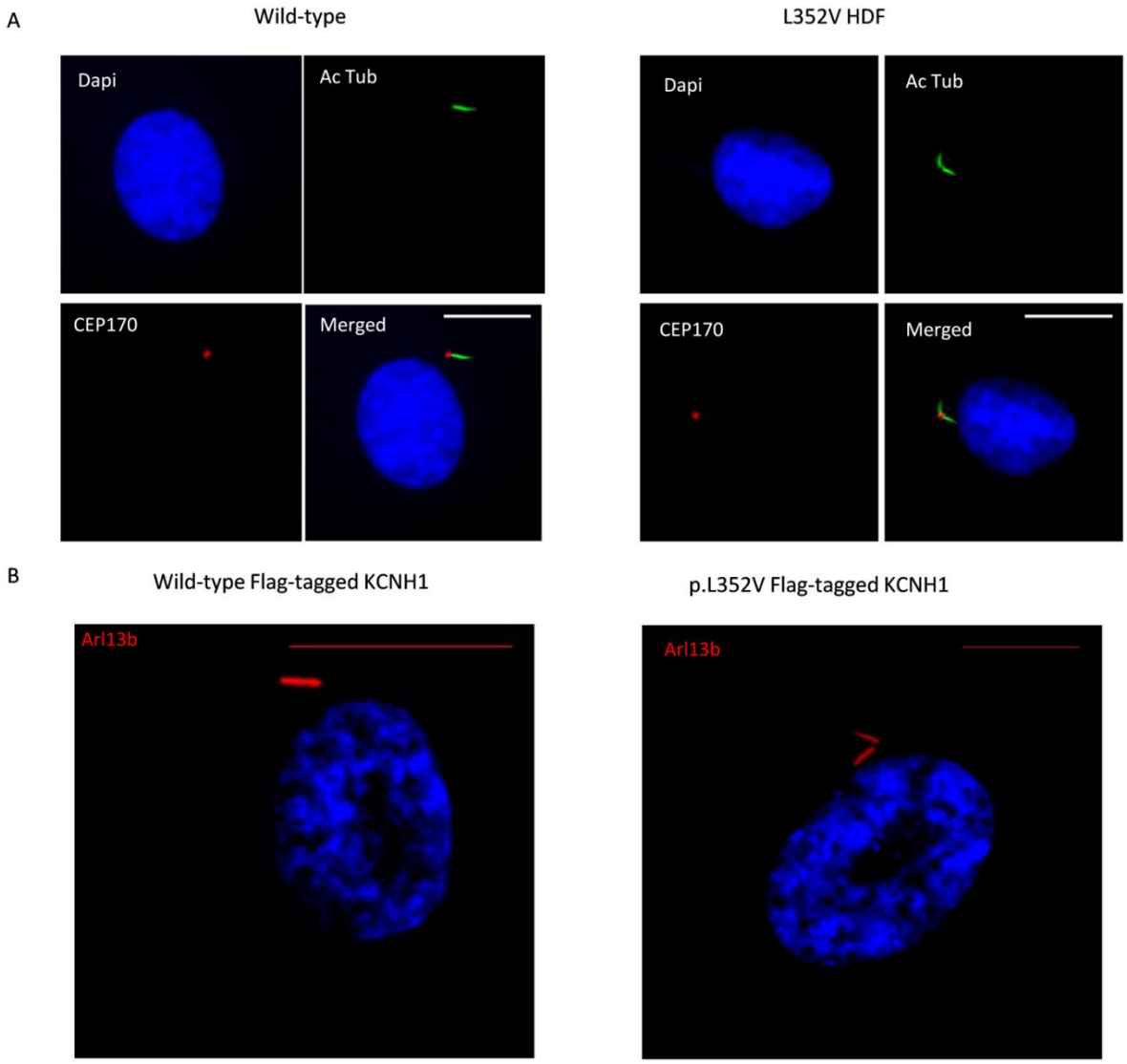

Figure 16. KCNH1 p.L352V variant leads to multiple cilia formation.

A. Immunofluorescence microscopy of ciliated wild-type and p.Leu352Val KCNH1 patient's fibroblasts stained with antibodies to acetylated alpha tubulin (green) and CEP170 (red). DNA was visualized with DAPI (blue). ZLS patient's fibroblasts exhibit multi ciliated cells. Scale bar: 10µm.

B. Immunofluorescence microscopy of ciliated hTERT RPE-1 cells transfected with plasmid expressing KCNH1 Flag tagged expressing wild type and p.Leu352Val mutant protein. The staining was performing using anti-Arl13b (red) antibody and DNA was visualized with DAPI (blue). hTERT RPE-1 cells transfected with p.Leu352Val Flag-tagged KCNH1 shows multiciliation. Scale bar: 10µm.

The structure anomalies of p.Arg330Gln cilia cells led to analyse the steady-state localization of the IFT172, a member of the IFT-B complex involved in the anterograde transport of cargo in the cilium (Gorivodsky et al., 2009). After 48h serum starvation, IFT172 was found almost exclusively at the base of the cilia in wild-type fibroblasts but in a proportion of p.Arg330Gln and p.Leu352Val fibroblasts at both the base and tip of the cilia (Figure 17). This bulbous morphology suggests impaired retrograde transport.

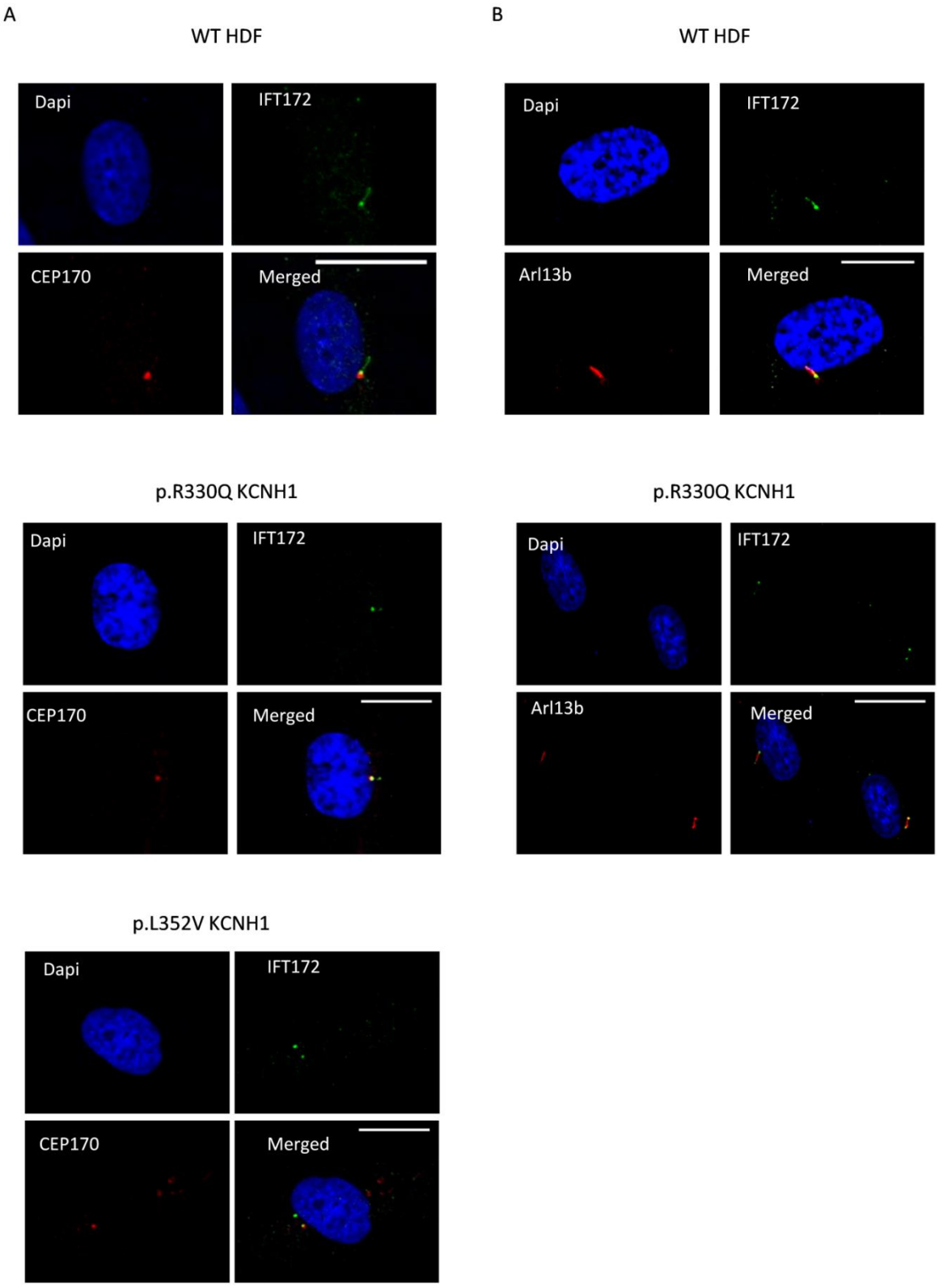

Figure 17. Impaired ciliary transport in ZLS patients' fibroblasts.
Immunofluorescence microscopy of ciliated wild type and ZLS patient's fibroblasts stained with IFT172 (green) and CEP170 (red, A) or Arl13b (red, B). DNA was visualized with DAPI (blue). Scale bar: 10µm.

4.7 KCNK4 sub-cellular localization

Immunofluorescence assays were performed to eventually localize KCNK4 to the primary cilium, using alpha acetylated tubulin and KCNK4 specific antibody in HDF and hTERT RPE-1 cell lines.

As shown in Figure18 we did not observe localization of the K^+ channel at the primary cilium. However, we could appreciate an unexpected nuclear localization of the protein in both HDF and hTERT RPE-1 cells, possibly indicating unrevealed roles of KCNK4.

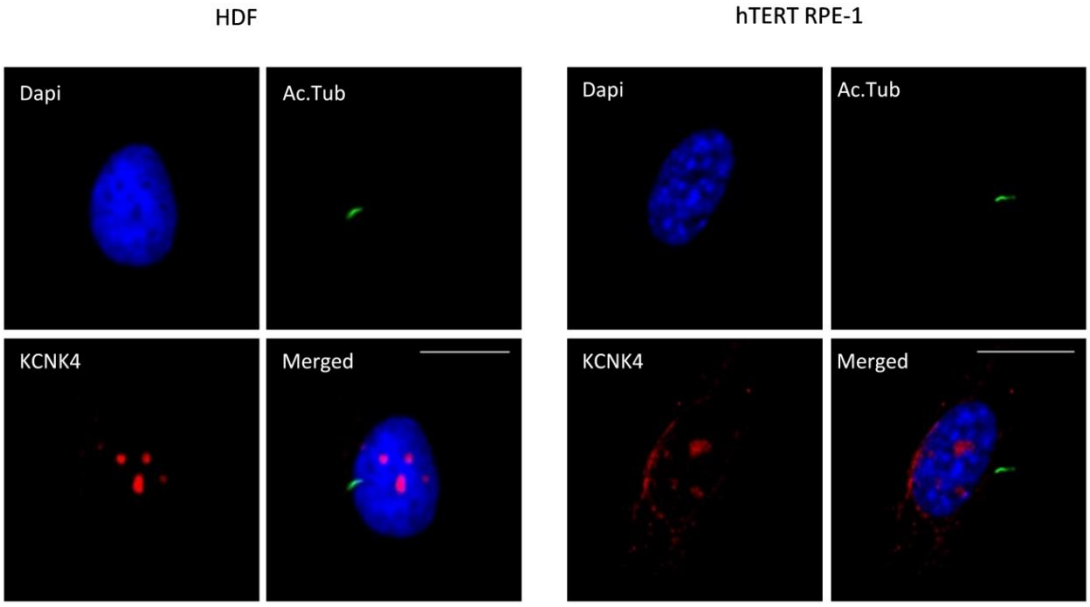

Figure 18. Nuclear Localization of KCNK4.
Representative immunofluorescence microscopy images of HDF and hTERT RPE-1 cells stained with anti-KCNK4 and anti-alpha acetylated tubulin antibodies. The panel evidence a nuclear localization of KCNK4. Scale bar: 10µm.

To confirm this observation, we performed co-localization experiments with Lamin A/C, as a nuclear envelope marker, and Fibrillarin, as a nucleolus marker, using double staining with antibodies in wild-type HDF and hTERT RPE-1 cells. A significant level of co-localization was observed with Fibrillarin antibody in the nucleoli of HDF and hTERT RPE-1 cells (Figure 19).

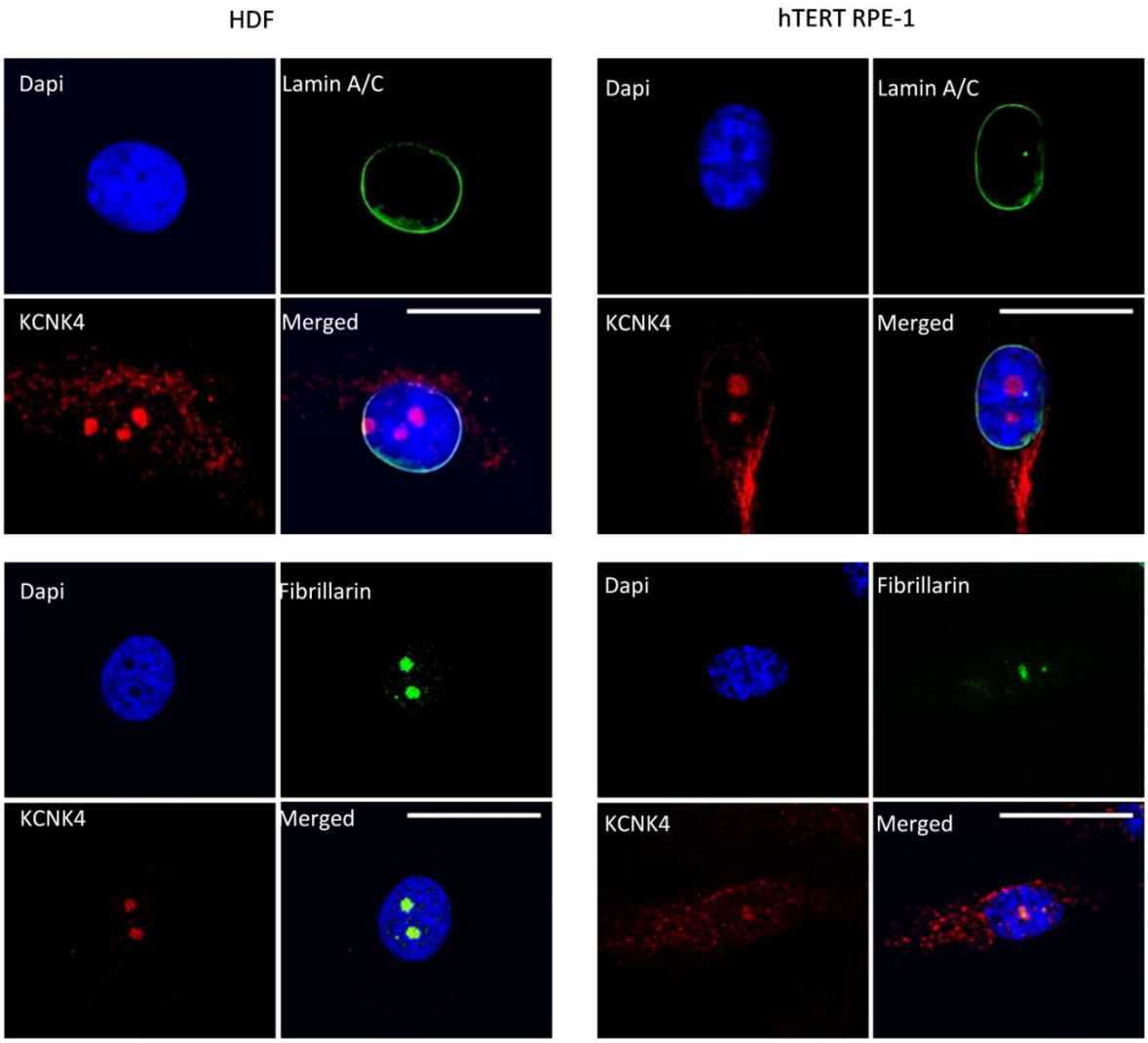

Figure 19. Nucleolar localization of KCNK4 protein.
HDF and hTERT RPE-1 cells were stained with anti-KCNK4 (red) and anti- Lamin A/C or Fibrillarin (green) antibodies. DNA was visualized with DAPI (blue). KCNK4 co-localizes with nucleolar marker Fibrillarin. Scale bar: 10µm.

4.8 Localization of KCNK4 during cell cycle

We used the localization of Ki-67, a nuclear protein associated with cell proliferation and nucleoli, at the main cell cycle stages of hTERT RPE-1 cells, to evaluate KCNK4 localization during cell cycle. As shown in Figure 20A Ki-67 mainly localized in the nucleoli during the G1, S, and G2 phases and during late G2 and early prophase. When the nucleoli disassemble, the protein is diffusely distributed in the nucleoplasm. In contrast to cycling cells, quiescent cells do not express Ki-67 (Solovei et al., 2006). We performed co-immunofluorescence experiments with Ki-67 antibody, to recognize the different cell cycle phases of hTERT RPE-1 cells. As shown in figure 20B, we observed partially co-localization between KCNK4 and Ki-67 during the G1 phases and a completely co-localization during the S and G2 phases, according with previously

results showing its nucleolar localization. Interesting, the G0 cells, which did not express Ki-67, showed a strong accumulation of KCNK4 in defined nuclei foci.

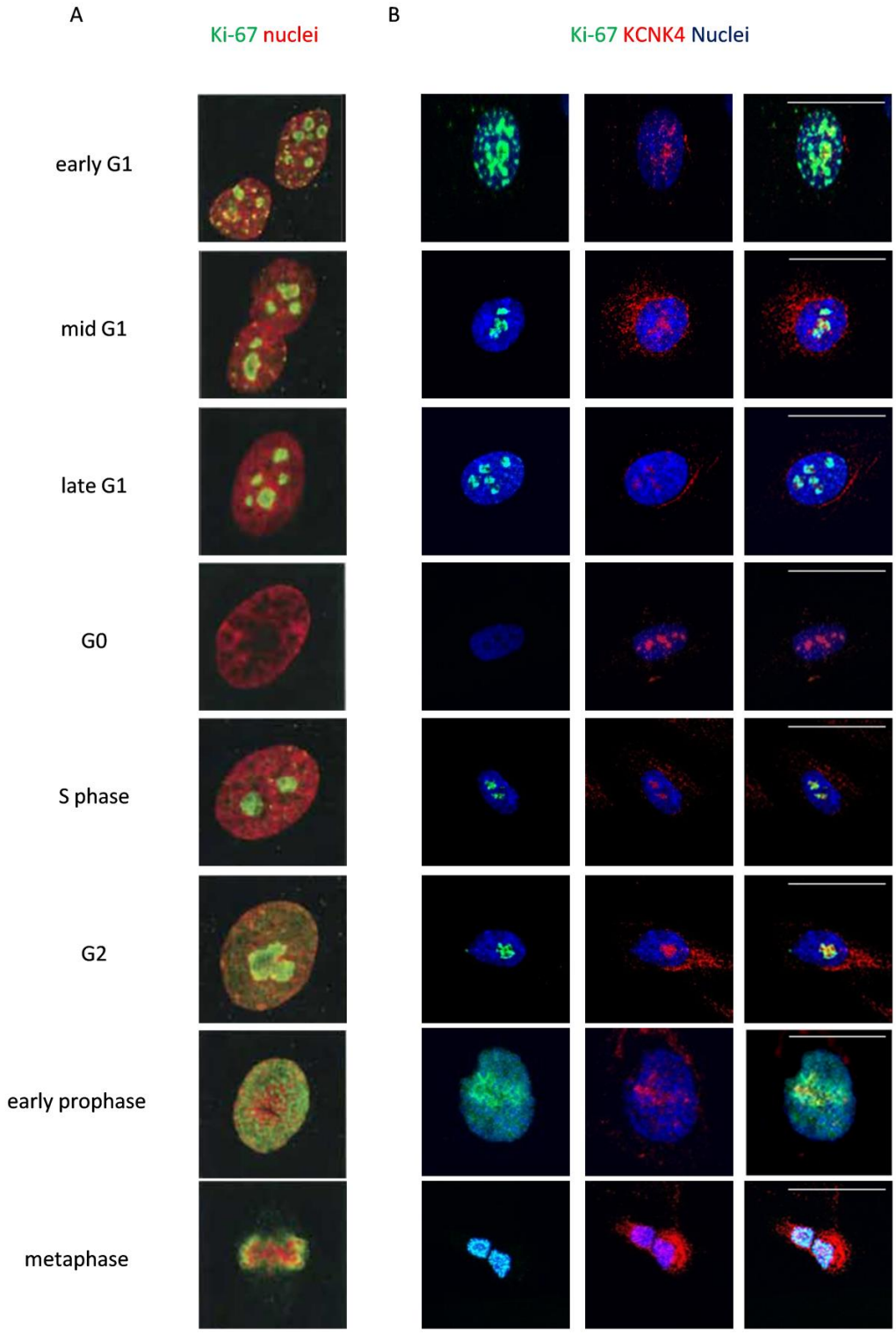

Figure 20. Localization of KCNK4 during cell cycle phases.
A. Immunostaining of Ki-67 during cell cycle of HDF. Modified from Soloveiet al., 2006.
B. Representative immunofluorescence microscopy images of hTERT RPE-1 cells stained with anti-KCNK4 and anti-Ki67 antibodies. The panel shows a nucleoli localization of KCNK4 in G1, S and G2 phases and an accumulation in G0 phase. Nuclei were visualized with DAPI (blue). Scale bar: 10µm.

5. DISCUSSION

K^+ channels are the most diverse group of ion channels. They control the K^+ flux through the cell membrane in response to multiple signals to modulate membrane potential and participate to many cell processes of both excitable and non-excitable cells. They are also key players in regulating cell excitability, cell volume, proliferation, apoptosis and cell cycle (Bauer et al., 2018).

Most functional studies on K^+ channels focused on their electrophysiological properties. Notably, while electrophysiological studies were performed to shed light on the mechanisms underlying KCNH1 and KCNK4 mutations in ZLS and FHEIG, no functional data have been collected on the consequences of mutations on cell functions, i.e. localization, structure, and altered pathways. Based on these considerations, we explored the functional impact of two KCNH1 mutations associated with ZLS (p.Arg330Gln and p.Leu352Val; Kortüm et al., 2015) and two KCNK4 mutations associated FHEIG (p.Ala244Pro and p.Ala172Glu; Bauer et al., 2018) using cellular approaches.

The transmembrane potential has been reported as a cellular bioelectric parameter that influences the progression through the cell cycle. K^+ channels have been implicated in the control of cell-cycle progression both through their influence on the membrane potential and through non-canonical permeation-independent mechanisms, showing remarkable cell cycle-dependent variations of expression and activity (Urrego et al., 2014). With the aim to investigate the functional impact of KCNH1 and KCNK4 mutations on cell cycle, we performed a proliferation assay by using primary fibroblasts as a cell model. Growth curve was carried out on control fibroblasts and on primary skin fibroblasts of patients with KCNH1-missense mutations p.Leu352Val causing ZLS (Kortüm et al., 2015), p.Arg330Glncausing ZLS (not published), SID (Bramswing et al., 2015) and SDDHS (Fukai et al., 2016) and with KCNK4-missense mutations (p.Ala244Pro and p.Ala172Glu) causing FHEIG (Bauer et al., 2018). We demonstrated that the mutations p.Arg330Gln in KCNH1 and p.Ala172Glu in KCNK4 did not impair cell proliferation. Differently, fibroblasts from patients carrying the p.Leu352Val substitution in KCNH1 and p.Ala244Pro in KCNK4 exhibited a very low proliferation rates compared to control fibroblasts, highlighting that both channels have a role in the regulation of cell proliferation. However, we showed that only one of the two analyzed mutations for both KCNH1 (p.Leu352Val) and KCNK4 (p.Ala244Pro) channels affect proliferation. One explanation could be that both KCNH1 p.Arg330Gln and KCNK4 p.Ala172Glu mutated proteins, when expressed in heterozygous state, may not be enough to observe a robust effect. Moreover, p.Leu352Val substitution map in the S5 helices and p.Arg330Gln in the voltage-sensing domain (S4 helix) of KCNH1 channel (Kortüm et al., 2015; Bramswig et al., 2015), and this different location would have a different impact on the proper cellular functions. In order to get better insight on this aspect and assess the functional role of K^+ channels in cell proliferation we plan to perform additional experiments by using transfected cells overexpressing KCNH1 and KCNK4 carrying all mutations reported as pathogenetic (Kortüm et al., 2015; Bauer et al., 2018).

Additionally, it is known that KCNH1 activity is cell cycle regulated, suggesting that it is likely involved in fundamental cellular and developmental processes (Urrego et al., 2014). KCNH1 is considered a bi-

functional protein that not only regulates K^+ flux but also intracellular signalling pathways, by mechanisms independent of K^+ ion flux. The effect of KCNH1 on intracellular signalling was evident as the non-conducting mutants in open conformation fail to influence proliferation (Hegle et al., 2006). Structural analysis predicted that p.Leu352Val substitutions might affect the closed-open transition forming a tight hydrophobic cluster with other residues in the open structure which rearranges in the closed conformation (Kortüm et al., 2015). Moreover, electrophysiological studies have shown the functional consequences of the p.Leu352Val KCNH1 mutation on channel activity, which shifted in the activation threshold to more negative potentials and slower deactivation compared to the wild-type channel (Kortüm et al., 2015). Differently, no electrophysiological data have been collected for p.Arg330Gln KCNH1 variation, which may not have the same gain of function effect. Here, we hypothesized that p.Leu352Val KCNH1 channels display a more open conformation which results in failure of proliferation induction. The decreased proliferation rate of fibroblasts from patients carrying the p.Leu352Val substitution in KCNH1 and p.Ala244Pro in KCNK4 observed in our experiments suggests the occurrence of cell cycling defects introduced by these KCNH1 and KCNK4 missense mutations. To date, while several studies have demonstrated that KCNH1 plays an active role in cell cycle progression in both cancer and non-transformed cells, no data have been collected for KCNK4. Our results on mutated primary fibroblasts corroborate the role of KCNH1 as a mediator of proliferation of non-transformed cells and highlight a function for KCNK4 in regulation of cell proliferation.

Control of cell cycle has been associated with ciliogenesis (Malicki et al., 2017). In tissues, quiescent cells assemble a primary cilium, an antenna-like sensory organelle that regulates multiple cell signalling pathways during development and in the adulthood (Morthorst et al., 2018). Cilia are dynamically regulated during cell cycle progression because assembly of the primary cilium requires a mature mother centriole: present in G0 and G1 and usually in S/G2 cells, but almost invariably resorbed before mitotic entry (Urrego et al., 2017). Mutations in genes that impair ciliary biogenesis, protein trafficking and function lead to a dysregulated signalling and cause diseases known as ciliopathies, which may affect nearly all organs during development or in adulthood (Urrego et al., 2017). It has been suggested that some clinical features of ZLS patients, as orofacial and digital abnormalities, together with severe mental retardation and morphological features, are at least in part reminiscent of ciliopathies (Sánchez et al., 2016). To evaluate whether KCNH1 (p.Arg330Gln and p.Leu352Val) mutations are associated with defects in assembly or disassembly of the primary cilium, we performed functional studies by using cell models.

Ciliogenesis assay was performed by immunofluorescence analysis in control and ZLS (KCNH1 p.Arg330Gln and p.Leu352Val) patients fibroblasts. We found a significant increase of cilia frequency in all the analyzed patients fibroblasts compared to control in cycling condition, before the induction of quiescent state by serum starvation, thus suggesting a functional role of KCNH1 in ciliogenesis. As K^+ channels expression is not constant in all phases of the cell cycle, we might speculate that a significant fraction of mutant fibroblasts are in a different phase of cell cycle in cycling condition, possibly G0, compared to control fibroblasts. It was also observed that, upon reintroduction of serum, to induce cilium disassembly, the number of ciliated cells increase in fibroblasts with p.Leu352Val KCNH1 mutation. In

contrast, fibroblasts of p.Arg330Gln KCNH1 mutation did not show any difference in timing of cilium disassembly.

In cells synchronized in G0, a first resorption wave starts shortly after stimulation by serum (1-2 hours), when G1 phase starts, and a second wave occurs when entry into mitosis (18-24 hours) (Urrego et al., 2017). We would speculate that fibroblasts derived from patients carrying gain of function mutations in KCNH1 were more vulnerable to altered channels and would have a delay in ciliary resorption after reinitiating of the cell cycle. Therefore, we hypothesized that this channel may be implicated in either of the two waves of ciliation. To evaluate this aspect, experiments to analyze mutation effects on the second wave will be carried out.

KCNH1 accelerates ciliary disassembly and KCNH1-knockout (KO) cells maintain their cilia for significantly longer periods than wild-type cells (Sanchez et al., 2016). Of note, in fibroblasts carrying p.Leu352Val mutation in KCNH1 we observed similar effects to KCNH1-KO on the number of ciliated cells. These results were consistent with their decreased proliferation ability, suggesting that both the increase in ciliated cells and the decrease in proliferation could directly be attributable to the alteration of KCNH1 function.

We evaluated if the pathogenic mechanism of mutants KCNH1 could rely on altered channel ciliary localization. To this aim, microscopy experiments were performed in ZLS patient's-derived fibroblasts and in transfected cell lines. Previous studies localized KCNH1 in mammalian cells at the plasma membrane and intracellular structures, including the inner nuclear membrane, endocytic vesicles and primary cilium base (Sanchez et al.,2016). Our electron microscopy experiments performed in wild-type hTERT RPE-1 cells not only confirmed the localization at the plasma membrane and endocytic vesicles but also highlighted channel localization in the Golgi apparatus. Moreover, immunofluorescence analysis refined the reported KCNH1 localization in the cilium to be concentrated at the centrosome and ciliary pocket regions of both wild-type fibroblasts and hTERT RPE-1 cells. In particular, we demonstrated that KCNH1 co-localized with CEP164, a distal appendage centrosome marker, and for the first time, with EHD, a ciliary pocket marker. Moreover, we found co-localization with Rab5, an early endosomes marker. Microscopy analysis conducted on fibroblasts derived from the subjects carrying the KCNH1 p.Arg330Gln and p.Leu352Val changes, showed the same wild-type channel distribution for mutants KCNH1. This result was also confirmed in transfected hTERT RPE-1 cells. Many cell types, including fibroblasts and RPE-1 cells, contain an invagination of the periciliary membrane known as the ciliary pocket, which mediates ciliary endocytic activity and vesicular trafficking and is involved in basal body positioning and signal transduction. It is connected to the basal body through the distal appendages which anchor the mature mother centriole to the plasma membrane through centrosomal proteins, such as CEP164, which are essential not only for vesicle docking but also for the recruitment of IFT machinery (Malicki et al., 2017).

Given the ciliary localization of both wild-type and mutants KCNH1, we evaluated the effect of mutations of KCNH1 on the function and morphology of primary cilia. We studied primary cilia morphology of KCNH1 mutants, on ZLS patient's fibroblasts and transiently transfected hTERT RPE-1 cell lines, disclosing

some altered morphology. Some p.Leu352Val fibroblasts showed multi-ciliated cells, whereas a proportion of p.Arg330Gln fibroblasts cilia exhibited axoneme breaks and bulbous tips. These results were confirmed also in transfected RPE-1 cells. Bulbous tip suggested a defect in the ciliary transport. Ciliary protein transport is mediated by IFT machinery which consist of two large protein complexes, IFT-A and IFT-B, involved in retrograde and anterograde transport (Morthorst et al., 2018). We demonstrated that morphological abnormal cilia in both ZLS affected fibroblasts showed a significant accumulation of IFT172, involved in anterograde transport, at the ciliary tip. This bulbous morphology has already been observed in several cilia-related mutants and is thought to represent impaired retrograde transport (Shaheen et al., 2019; Shah et al., 2015; Tsao et al., 2008).

The development of most human organs depends on correct signal transduction within the primary cilium, and the right assembly/disassembly of the organelle. IFT transports axonemal precursors and signalling proteins along the length of the cilium. This mechanism is essential for maintenance of cilia structure but also for the regulation of cilia-mediated signalling pathways such as SHH, WNT, and TGF (Goetz et al., 2010). To this aim, we studied components of cilium related pathways, as the SHH pathway, that is mainly related to determination of cell fate and morphogenesis (Morthorst et al., 2018). To test the SHH pathway activation we determined the abundance of mRNA of *BCL2*, *PTCH1* and *SMO*, genes. Real-time PCR was carried out in cycling control fibroblasts and in fibroblast derived from patients with p.Arg330Gln and p.Leu352Val *KCNH1* mutations. We observed up-regulation of basal expression levels of SHH target genes *BCL2* and *PTCH1* in all ZLS fibroblasts, without ligand stimulation, suggesting that this pathway is hyperactive at basal level. In contrast, we did not observe a significant variation of *SMO* mRNA levels. It is known that, in the absence of SHH ligand, Sufu negatively regulates the pathway activation by forming a complex with Gli proteins at cilia tips and the downstream Gli transcription factors are processed at the primary cilium to render their repressor forms (He et al., 2014). One explanation of ectopic activation of the pathway in KCNH1 mutant fibroblasts could be related to a mislocalization of Gli/Sufu complexes away from the ciliary tip, where they became inappropriately activated in the absence of ligand, or to the ectopic Smo transport into the cilia. Moreover, it is known that the increased number of cilia reinforce activation of SHH pathway (Sánchez et al., 2016). Hence, the basal SHH hyperactivation in ZLS fibroblasts might results from the amount of ciliation. We suggest that observed altered SHH activation could be a consequence of dysfunction of cilia trafficking. Furthermore, structural abnormalities were detected in fibroblasts from KCNH1 p.Leu352Val patient, including several cells with multiple cilia. We considered that multiple primary cilia might cause changes in signalling pathways that rely on cilium function, including SHH. In summary, we might speculate that p.Arg330Gln and p.Leu352Val mutations in *KCNH1* cause different alteration on primary cilium morphology which may partially converge to the same pathways, as IFT transport and SHH pathways. Additionally, we confirmed upregulation of BCL2 also at protein level by western blot analysis in p.Leu352Val KCNH1 mutated fibroblasts. It is known that the anti-proliferative function of BCL2 facilitates G0 arrest (Zinkel et al., 2006). Our results on BCL2 overexpression corroborated previous results obtained in fibroblasts carrying p.Leu352Val KCNH1 mutations, which showed impaired

proliferation capability. Impaired ciliary SHH signalling has also been reported in mouse embryonic fibroblasts obtained from KCNH1-KO (Sánchez et al., 2016). Interestingly, we observed that KCNH1-KO and p.Leu352Val mutations showed very similar effects on SHH pathway activation. In summary, our findings supported the hypothesis that the alteration of KCNH1 resulting in impaired ciliary formation affect also ciliary functioning at least in part through SHH signalling.

The ciliary localization of mutant KCNH1 suggests that impaired ciliogenesis and morphology could rely from altered function of KCNH1 at the primary cilium base. We can speculate that KCNH1 induce changes of membrane potential and consequent change in local Ca^{2+} levels around the ciliary pocket or the base of the cilium, a phenomenon that has been long known to be important for deciliation (Urrego et al., 2017). Local changes in potential would influence $Ca2^{+}$ entry, that is a crucial modulator of deciliation (Sanchez et al., 2016) and the phospholipid composition of the membrane, which influences the competence of the permeation barrier at the transition zone of the primary cilium (Urrego et al 2017). Mutant proteins could have altered function in regulating this fine-tuned mechanism, and this could also explain the impairment of ciliary transport or improper activation of SHH pathway of ZLS mutants.

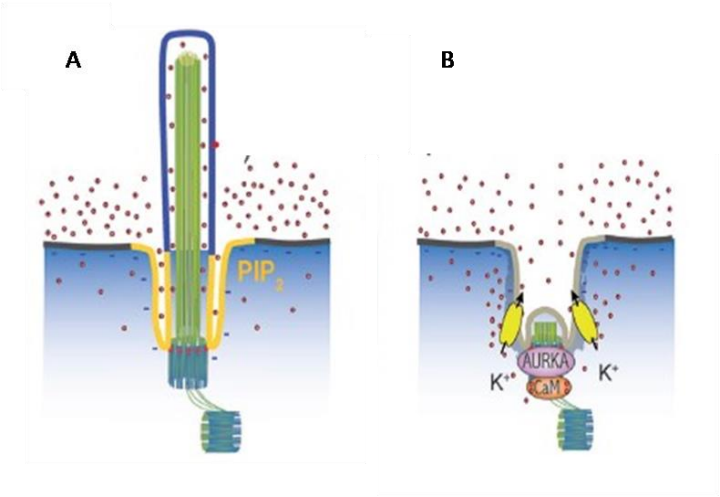

Figure 21. Schematic representation of KCNH1 role in primary cilium disassembly.
In quiescent ciliated cells, intracellular $Ca2^{+}$ is very low and PIP2 is concentrated at the base of the cilium. When KCNH1 starts its expression, the membrane potential is hyperpolarized, allowing for $Ca2^{+}$ enrichment and PIP2 disaggregation (brown colour) at the ciliary membrane. $Ca2^{+}$ binds to CaM and thereby activates AURKA, and lower PIP2 concentration allows ciliary membrane proteins to diffuse back to the plasma membrane, resulting in ciliary resorption. Modified from Urrego et al., 2017.

Twelve different gain-of-function KCNH1 mutations have been identified in twenty-three patients with ZLS, TMBTS, SID and SDHHS diagnosis (Figure 22). Despite these identified KCNH1 mutated patients could not be assigned to the same syndrome, a comparison of them, allowed to disclose the presence of some shared clinical features, like intellectual disability, craniofacial dysmorphism, seizures and/or epilepsy, and hypoplastic nails. Sometimes the same mutation has been reported in association with different clinical diagnosis, providing the stronger evidence that these syndromes belong to a phenotypic continuum. It is the case of p.Gly348Arg and p.Ile467Val mutations, which were found in patients with ZLS and TMBTS syndromes, and p.Leu462Phe, which was found in both TMBTS and SID patients and p.Arg330Gln, which

has been reported in association with ZLS, SID and SDHHS patients. We studied the impact of Arg330Gln on KCNH1 cellular functions. Mutations in Arg330 residue have been identified in seven patients carrying KCNH1 mutations, suggesting that this mutation occur with higher frequency and should be recognized as a hotspot mutations in KCNH1-associated syndromes. Moreover, Arg330 residue was associated with two amino acid changes (p.Arg330Gln and p.Arg330Pro). The substitutions mapped in the voltage-sensing domain (S4 helix) of KCNH1 channel (Kortüm et al., 2015) which directly interacts with C-linker to induce a bent in S6 segment to close the channel under a hyperpolarized state. Hence, mutations could impede the movement of voltage sensor from the activated state thereby favoring the opening state and enhancing K^+ transporting function. The amount of K^+ transport may limit the opening of voltage-gated Na^+ and $Ca2^+$ channels, two major effectors during epilepsy, one of the main features of KCNH1 patients that was found associated with the gain-of-function of KCNH1. These mutations with gain-of-function compared to that in other K^+ channels with loss-of-function indicate that the mechanisms mediating the epileptic phenotype may be different from that in classical types of epilepsy. We also analyzed the functional impact of p.Leu352Val substitution. While the same p.Arg330Gln mutation has been reported in association with different clinical diagnosis, KCNH1 p.Leu352Val mutation was identified only in one patient with ZLS main features, as gingival hyperplasia, DD/ID, seizures, coarse face and hypoplastic nails and phalanges (Kortüm et al., 2015). p.Leu352 mapped in the S5 helices and structural analysis predicted that p.Leu352Val substitutions might affect the closed-open transition forming a tight hydrophobic cluster with other residues in the open structure which rearranges in the closed conformation (Kortüm et al., 2015). Moreover, electrophysiological studies have shown that mutant channels exhibited accelerated channel activation and slower deactivation, producing dramatic increases in whole cell K^+ conductance (Kortüm et al., 2015).

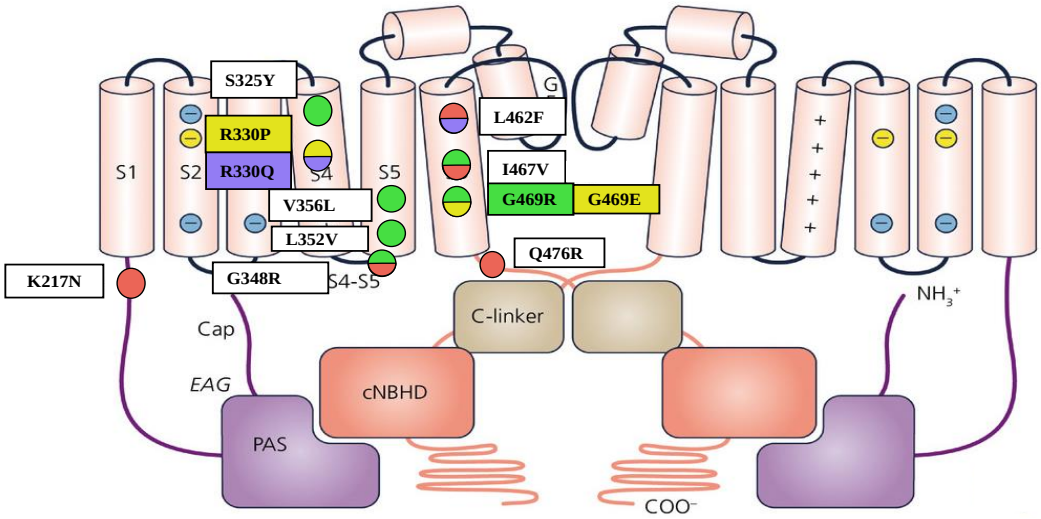

Figure 22. **Schematic representation of KCNH1 subunits and location of all identified mutations.**
In green mutations associated with ZLS, in red with TMBTS, in blue with SID and in yellow with SDDHS.

Given that patients with activating mutations in *KCNK4* showed major clinical features of ZLS subjects with gain-of-function mutations in *KCNH1*, one would hypothesize alteration related to impairment of convergent mechanisms as ciliogenesis in the presence of *KCNK4* mutations. We investigated the ciliogenesis potential of p.Ala172Glu and p.Ala244Pro KCNK4 FHEIG fibroblasts by performing the ciliogenesis assay. As for KCNH1 mutated fibroblasts, we found a significant increase of cilia frequency in all the analyzed patients fibroblasts compared to control in cycling condition, before the induction of quiescent state by serum starvation, thus suggesting a role of KCNK4 in regulation of ciliogenesis. If KCNH1 and KCNK4 are implicated in ciliogenesis, one would speculate a developmental phenotype in the presence of channels alteration related to impaired ciliogenesis. This is indeed the case for Temple–Baraitser, ZLS and FHEIG syndromes, recently identified as gain-of-function mutations in KCNH1 and KCNK4 (Simons et al., 2015; Kortüm et al., 2015; Bauer et al.,2018). Given that K^+ permeation is required for deciliation, the effect should be associated with changes in the local polarization of the membrane, which would influence $Ca2^+$ entry (Sanchez et al., 2016).

Given that fibroblasts from FHEIG patients showed proliferation and ciliogenesis impairment, we evaluated if KCNK4 channels localize at the primary cilium as KCNH1. To this aim, we performed immunofluorescence experiments on fibroblasts and hTERT RPE-1 cells demonstrating that KCNK4 did not localize at the primary cilium area. Of note, we disclosed a sub-cellular localization of the channel, in the nucleoli of both cell types. Several ion channels are found to localize in the nuclear region of cells, but the functional roles remain unclear (Jang et al., 2015). Although KCNK4 channels have been characterized using electrophysiological techniques, their presence in the nucleus has not been previously reported and we demonstrated it for the first time, to our knowledge. We speculated that, such as KCNH1, it might be a bi-functional protein whose non canonical functions might be closely linked to processes that occur inside the nucleolus. In addition to its role in ribosome biogenesis, the nucleolus acts as a critical stress sensor and coordinates downstream responses such as altered metabolism, differentiation, cell cycle arrest, autophagy, DNA repair, senescence, and apoptosis (Chen et al 2018). We also observed that hTERT RPE-1 cells exhibited a cell cycle dependent KCNK4 accumulation in nuclei foci, with a strong accumulation in G0 cells, clearly recognized by strongly down-regulation of proliferation marker Ki-67. These results were consistent with the hypothesis that mutations in *KCNK4* could influence cell cycle progression and that reduced proliferation and increased ciliogenesis observed in fibroblasts from FHEIG patients could rely from increase of cells in G0 phase. We plan sub-cellular fractioning experiments in order to confirm the nucleolar localization of the channel. Patients with activating mutations in *KCNK4* showed major clinical features of ZLS subjects with gain-of-function mutations in *KCNH1*. Despite KCNK4 didn't localize at the primary cilium, we evaluated the effects of p.Ala172Glu and Ala244Pro *KCNK4* mutations on the activity of SHH pathway. As for KCNH1, we observed upregulation of basal expression levels of SHH target genes *BCL2* and *PTCH1* in all FHEIG fibroblasts, without ligand stimulation, suggesting that this pathway is hyperactive at basal level. Additionally, we confirmed upregulation of BCL2 also at protein level by western blot analysis in fibroblasts from p.Ala244Pro KCNK4 patient.

Patients with activating mutations in *KCNK4*, show variable developmental delay and cognitive impairment and gingival overgrowth (Bauer et al., 2018), which are common feature of subjects with gain-of-function mutations in *KCNH1* (Kortüm et al., 2015). Recently, dominantly acting missense mutations in *KCNN3*, coding for a Ca^{2+}-activated K channels, were identified in three subjects with the major clinical features of ZLS (Bauer et al., 2019) and significant clinical overlap with KCNH1 ZLS- and KCNK4 FHEIG -related disorders (Kortüm et al., 2015; Bauer et al., 2018). With the identification of gain-of-function mutations in KCNN3, it was proposed to include the phenotypes associated with mutations in KCNH1, KCNK4, and KCNN3 in a subgroup of neurological K^+ channelopathies characterized by DD/ID, coarse facial features, and gingival hyperplasia as common findings and epilepsy, hypertrichosis, and nail aplasia or hypoplasia as variable manifestations (Bauer et al., 2019), associated with an increase in K^+ conductance, especially evident at negative membrane potentials (Kortüm et al., 2015; Bauer et al., 2018; Bauer et al., 2019).

In summary, our results highlighted a key role of KCNH1 and KCNK4 in the regulation of proliferation of non-transformed cells and suggest that both channels are involved in ciliogenesis and SHH pathway. KCNH1 and KCNK4 proteins showed different sub-cellular localization, and both localized in specific sensor compartments, highlighting that they would have specific ion channel-independent function converging on some cell pathways whose alteration might affect development processes, including proliferation, regulation of cell cycle and ciliogenesis and primary cilia pathways. This would explain the clinical features overlapping ZLS and FHEIG diseases.

Understanding the molecular bases of ZLS and related disorders and delineating more precisely genotype-phenotype correlations are key requisites to treat these diseases effectively. These disorders, which result from molecular alterations of different but possibly partially converging cellular pathways, overlap as regards to neurodevelopment and other developmental issues. Hence, treating these diseases requires a deeper knowledge of the signaling dysregulation associated to the pathogenesis and of the specific alterations caused by each affected protein. Our study might contribute to highlight the pathogenesis of these disorders and might address future studies with the aim of developing therapeutic strategies to ameliorate evolutive aspects of these diseases.

REFERENCES

Bauer CK, Schwarz JR. Ether-à-go-go K (+) channels: effective modulators of neuronal excitability. J Physiol. 2018

Bauer CK, Calligari P, Radio FC, Caputo V, Dentici ML, Falah N, High F,Pantaleoni F, Barresi S, Ciolfi A, Pizzi S, Bruselles A, Person R, Richards S, Cho MT, Claps Sepulveda DJ, Pro S, Battini R, Zampino G, Digilio MC, Bocchinfuso G, Dallapiccola B, Stella L, Tartaglia M. Mutations in KCNK4 that Affect Gating Cause a Recognizable Neurodevelopmental Syndrome. Am J Hum Genet. 2018

Bauer CK, Schneeberger PE, Kortüm F, Altmüller J, Santos-Simarro F, Baker L,Keller-Ramey J, White SM, Campeau PM, Gripp KW, Kutsche K. Gain-of-Function Mutations in KCNN3 Encoding the Small-Conductance Ca(2+)-Activated K(+) Channel SK3 Cause Zimmermann-Laband Syndrome. Am J Hum Genet. 2019

Bramswig NC, Ockeloen CW, Czeschik JC, van Essen AJ, Pfundt R, SmeitinkJ, Poll-The BT, Engels H, Strom TM, Wieczorek D, Kleefstra T, Lüdecke HJ. 'Splitting versus lumping': Temple-Baraitser and Zimmermann-Laband Syndromes. Hum Genet.2015

Cázares-Ordoñez V, Pardo LA. Kv10.1 potassium channel: from the brain to the tumors. Biochem Cell Biol. 2017

Chen J, Stark LA. Crosstalk between NF-κB and Nucleoli in the Regulation of Cellular Homeostasis. Cells. 2018

Chiamvimonvat N, Chen-Izu Y, Clancy CE, Deschenes I, Dobrev D, Heijman J, Izu L, Qu Z, Ripplinger CM, Vandenberg JI, Weiss JN, Koren G, Banyasz T, Grandi E, Sanguinetti MC, Bers DM, Nerbonne JM. Potassium currents in the heart: functional roles in repolarization, arrhythmia and therapeutics. J Physiol. 2017

Djillani A, Mazella J, Heurteaux C, Borsotto M. Role of TREK-1 in Health and Disease, Focus on the Central Nervous System. Front Pharmacol. 2019

Fink M, Lesage F, Duprat F, Heurteaux C, Reyes R, Fosset M, Lazdunski M. Aneuronal two P domain K+ channel stimulated by arachidonic acid and polyunsaturated fatty acids. EMBO J. 1998

Fukai R, Saitsu H, Tsurusaki Y, Sakai Y, Haginoya K, Takahashi K, Hubshman MW, Okamoto N, Nakashima M, Tanaka F, Miyake N, Matsumoto N. De novo KCNH1 mutations in four patients with syndromic developmental delay, hypotonia and seizures. J Hum Genet. 2016

Goetz SC, Anderson KV. The primary cilium: a signaling centre during vertebrate development. Nat Rev Genet. 2010

Gorivodsky M, Mukhopadhyay M, Wilsch-Braeuninger M, Phillips M, Teufel A, Kim C, Malik N, Huttner W, Westphal H. Intraflagellar transport protein 172 is essential for primary cilia formation and plays a vital role in patterning the mammalian brain. Dev Biol. 2009

Haitin Y, Carlson AE, Zagotta WN. The structural mechanism of KCNH-channel regulation by the eag domain. Nature. 2013

Han B, Tokay T, Zhang G, Sun P, Hou S. Eag1 K(+) Channel: Endogenous Regulation and Functions in Nervous System. Oxid Med Cell Longev.2017

He M, Subramanian R, Bangs F, Omelchenko T, Liem KF Jr, Kapoor TM, AndersonKV. The kinesin-4 protein Kif7 regulates mammalian Hedgehog signalling by organizing the cilium tip compartment. Nat Cell Biol. 2014

Hegle AP, Marble DD, Wilson GF. A voltage-driven switch for ion-independent signaling by ether-à-go-go K+ channels. Proc Natl Acad Sci U S A. 2006

Huang H, Li H, Shi K, Wang L, Zhang X, Zhu X. TREK-TRAAK two-pore domain potassium channels protect human retinal pigment epithelium cells from oxidative stress. Int J Mol Med. 2018

Huang X, Jan LY. Targeting potassium channels in cancer. J Cell Biol. 2014

Jang SH, Byun JK, Jeon WI, Choi SY, Park J, Lee BH, Yang JE, Park JB, O'Grady SM, Kim DY, Ryu PD, Joo SW, Lee SY. Nuclear localization and functional characteristics of voltage-gated potassium channel Kv1.3. J Biol Chem. 2015

Kortüm F, Caputo V, Bauer CK, Stella L, Ciolfi A, Alawi M, Bocchinfuso G, Flex E, Paolacci S, Dentici ML, Grammatico P, Korenke GC, Leuzzi V, Mowat D, Nair LD, Nguyen TT, Thierry P, White SM, Dallapiccola B, Pizzuti A, Campeau PM, Tartaglia M, Kutsche K. Mutations in KCNH1 and ATP6V1B2 cause Zimmermann-Laband syndrome. Nat Genet. 2015

Kukic I, Rivera-Molina F, Toomre D. The IN/OUT assay: a new tool to study ciliogenesis. Cilia. 2016

Malicki JJ, Johnson CA. The Cilium: Cellular Antenna and Central Processing Unit. Trends Cell Biol. 2017

Mastrangelo M, Scheffer IE, Bramswig NC, Nair LD, Myers CT, Dentici ML, Korenke GC, Schoch K, Campeau PM, White SM, Shashi V, Kansagra S, Van Essen AJ, Leuzzi V. Epilepsy in KCNH1-related syndromes. Epileptic Disord. 2016

Mégarbané A, Al-Ali R, Choucair N, Lek M, Wang E, Ladjimi M, Rose CM, Hobeika R, Macary Y, Temanni R, Jithesh PV, Chouchane A, Sastry KS, Thomas R, Tomei S, Liu W, Marincola FM, MacArthur D, Chouchane L. Temple-Baraitser Syndrome and Zimmermann-Laband Syndrome: one clinical entity? BMC Med Genet. 2016

Morthorst SK, Christensen ST, Pedersen LB. Regulation of ciliary membrane protein trafficking and signalling by kinesin motor proteins. FEBS J. 2018

Noël J, Sandoz G, Lesage F. Molecular regulations governing TREK and TRAAK channel functions. Channels (Austin). 2011

Park SM, Jang HJ, Lee JH. Roles of Primary Cilia in the Developing Brain. Front Cell Neurosci. 2019

Ramos Gomes F., Romaniello V., Sánchez A., et al. Alternatively spliced isoforms of Kv10.1 potassium channels modulate channel properties and can activate cyclin-dependent kinase in Xenopus oocytes. The Journal of Biological Chemistry. 2015

Sánchez A, Urrego D, Pardo LA. Cyclic expression of the voltage-gated potassium channel KV10.1 promotes disassembly of the primary cilium. EMBO Rep.2016

Serrano-Novillo C, Capera J, Colomer-Molera M, Condom E, Ferreres JC, Felipe A. Implication of Voltage-Gated Potassium Channels in Neoplastic Cell Proliferation. Cancers (Basel). 2019

Shah AS, Farmen SL, Moninger TO, Businga TR, Andrews MP, Bugge K, Searby CC, Nishimura D, Brogden KA, Kline JN, Sheffield VC, Welsh MJ. Loss of Bardet-Biedl syndrome proteins alters the morphology and function of motile cilia in airway epithelia. Proc Natl Acad Sci U S A. 2008

Shaheen R, Jiang N, Alzahrani F, Ewida N, Al-Sheddi T, Alobeid E, Musaev D, Stanley V, Hashem M, Ibrahim N, Abdulwahab F, Alshenqiti A, Sonmez FM, Saqati N, Alzaidan H, Al-Qattan MM, Al-Mohanna F, Gleeson JG, Alkuraya FS. Bi-allelic Mutations in FAM149B1 Cause Abnormal Primary Cilium and a Range of Ciliopathy Phenotypes in Humans. Am J Hum Genet. 2019

Shieh CC, Coghlan M, Sullivan JP, Gopalakrishnan M. Potassium channels: molecular defects, diseases, and therapeutic opportunities. Pharmacol Rev. 2000

Simons C, Rash LD, Crawford J, Ma L, Cristofori-Armstrong B, Miller D, RuK, Baillie GJ, Alanay Y, Jacquinet A, Debray FG, Verloes A, Shen J, Yesil G, GulerS, Yuksel A, Cleary JG, Grimmond SM, McGaughran J, King GF, Gabbett MT, Taft RJ. Mutations in the voltage-gated potassium channel gene KCNH1 cause Temple-Baraitser syndrome and epilepsy. Nat Genet. 2015

Solovei et al., 2006, Detection of Cell Cycle Stage in situ in Growin Cell Population, Cell Biology -Third Edition, A Laboratory Handbook Volume 1, Pages 291-299

Tian C, Zhu R, Zhu L, Qiu T, Cao Z, Kang T. Potassium channels: structures, diseases, and modulators. ChemBiol Drug Des. 2014

Tsao CC, Gorovsky MA. Tetrahymena IFT122A is not essential for cilia assembly but plays a role in returning IFT proteins from the ciliary tip to the cell body. J Cell Sci. 2008

Ufartes R, Schneider T, Mortensen LS, de Juan Romero C, Hentrich K, Knoetgen H, Beilinson V, Moebius W, Tarabykin V, Alves F, Pardo LA, Rawlins JN, Stuehmer W. Behavioural and functional characterization of Kv10.1 (Eag1) knockout mice. Hum Mol Genet. 2013

Urrego D, Tomczak AP, Zahed F, Stühmer W, Pardo LA. Potassium channels in cell cycle and cell proliferation. Philos Trans R Soc Lond B Biol Sci. 2014

Urrego D, Movsisyan N, Ufartes R, Pardo LA. Periodic expression of Kv10.1driven by pRb/E2F1 contributes to G2/M progression of cancer and non-transformed cells. Cell Cycle. 2016

Urrego D, Sánchez A, Tomczak AP, Pardo LA. The electric fence to cell-cycle progression: Do local changes in membrane potential facilitate disassembly of the primary cilium?: Timely and localized expression of a potassium channel may set the conditions that allow retraction of the primary cilium. Bioessays. 2017

Wang L, Dynlacht BD. The regulation of cilium assembly and disassembly indevelopment and disease. Development. 2018

Wang X, Chen Y, Zhang Y, Guo S, Mo L, An H, Zhan Y. Eag1 Voltage-Dependent Potassium Channels: Structure, Electrophysiological Characteristics, and Function in Cancer. J Membr Biol. 2017

Wynia-Smith SL, Gillian-Daniel AL, Satyshur KA, Robertson GA. hERG gating microdomains defined by S6 mutagenesis and molecular modeling. J Gen Physiol.2008

Zinkel S, Gross A, Yang E. BCL2 family in DNA damage and cell cycle control. Cell Death Differ. 2006